Journal of proteome research

pubs.acs.org/jpr

Article

Metabolic–Immuno–Hormonal Cross-talk in Breast Cancer: A UAE-Based Multi-Omics Perspective

Published as part of Journal of Proteome Research special issue "Multiomics in Africa and the Middle East".

Sarra B. Shakartalla, Sara Naif, Hamza M. Al-Hroub, Riyad Bendardaf, and Sameh S. M. Soliman*

Cite This: https://doi.org/10.1021/acs.jproteome.5c00669

Read Online

ACCESS | Metrics & More | Article Recommendations | Supporting Information

ABSTRACT: Breast cancer (BC) remains the leading cause of cancer-related death among women in the Middle East and North Africa, with particularly high mortality in the United Arab Emirates (UAE), mainly due to delayed diagnosis. This study aimed to identify metabolic and proteomic biomarkers associated with BC progression in the UAE population. A cohort of 35 BC patients and 30 healthy control (HC) individuals underwent plasma-based untargeted metabolomics and proteomics analyses using LC-QTOF-MS. Multivariate statistical models, including OPLS-DA and AUROC analyses, were employed to assess biomarker performance. Integrated pathway and structural motif analyses were conducted to explore disease-stage-specific signatures. A distinct metabolic signature was identified, featuring disrupted amino acid (particularly arginine), purine/pyrimidine, and steroid hormone metabolism. Key metabolites such as L-arginine, hypoxanthine, uridine, vitamin D3, and estradiol showed stage-specific alterations. Eleven metabolites yielded high diagnostic power (AUROC = 0.954). Structural motif analysis revealed a transition from small, polar metabolites in early-stage BC to complex, lipophilic steroidal, and lipid structures in late-stage disease. Integrated proteomics revealed dysregulated immune and hormonal signaling, highlighting the cross-talk among metabolic, immune, and endocrine pathways. This UAE-based study reveals distinct metabolic and structural features of BC progression, suggesting candidate biomarkers for BC detection and personalized therapy.

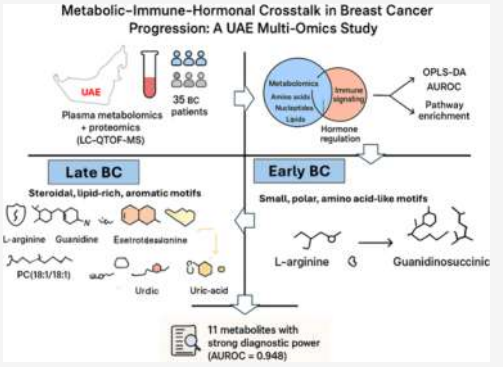

KEYWORDS: *breast cancer, metabolomics, proteomics, metastasis, UAE*

1. INTRODUCTION

Breast cancer (BC) remains the most commonly diagnosed malignancy among women globally, with approximately 2.29 million new cases reported in 2022, according to the latest statistics from the World Health Organization (WHO).[1] BC was recognized as the leading cause of cancer-related mortality among women in 2022, contributing to 15.4% (666,000 deaths) of all cancer-related deaths and preceding lung cancer.[1] The anticipated increase in mortality is suggested to reach 4 million by 2070.[2,3]

BC represents 43.9% of a five year cancer prevalence among women in the UAE.[1] In 2022, an estimated 1000 new cases were diagnosed in the UAE.[1] Despite the advances in awareness and treatment of BC, the disease still has the highest mortality rate among females in the UAE, constituting 25.3% of all cancer cases.[4] It should be emphasized that the Arab and Emirati populations exhibit distinct pathological and histological characteristics of BC compared with Western nations. This includes a notably earlier age of onset, higher grade, a higher prevalence of human epidermal growth factor receptor-2 (HER-2) overexpression in younger populations than older women, and less common BC gene 1 and 2 (BRCA1 and BRCA2) mutations.[5−7] In Arab populations, the average age of BC diagnosis is around 48 years, with about two-thirds of the cases occurring in women under the age of 50.[8] Over 75% of BC patients in the UAE seek medical advice after experiencing a symptom or sign of the disease, while many others wait until the disease is more advanced.[9]

Early diagnosis of BC is very crucial as the survival rate drops significantly from nearly 100% for in situ carcinoma to 85.5% for early-stage invasive carcinoma and 25% for metastatic conditions.[10] Despite the availability of numerous clinical and experimental imaging modalities exhibiting elevated sensitivity levels (exceeding 90%) in the diagnosis of symptomatic BC patients, an efficient diagnostic instrument for the identification of early-stage BC (stages I and II) remains elusive.[11,12] Consequently, a detection method that facilitates precise and

Received: August 24, 2025
Revised: January 27, 2026
Accepted: February 4, 2026

early diagnosis and screening, which ultimately results in timely intervention and improved BC survival rates, is of paramount importance.

Cancer cells reprogram their metabolism in order to sustain their rapid growth and survival, a trait known to be one of the hallmarks of cancer.[13] This metabolic reprogramming offers opportunity for biomarker discovery and provides new targets for tumor treatment. Metabolite screening provides a non-invasive and promising alternative option for the diagnosis and prognosis of early BC. Unlike proteomics or genomics, metabolomics refers to the downstream changes at the metabolic cell level, representing a dynamic end product of the biological metabolic process.[10] This not only makes the diagnosis and staging of cancer possible for most effective intervention, but also sheds light on tumor development, drug response, and drug resistance, ultimately enhancing patient care and outcome.[14] Multiple altered metabolic pathways including alanine, aspartate, and glutamate pathways, glutamine and glutamate metabolic pathways, and arginine biosynthesis pathways were critical in BC.[10] Fatty acid biosynthesis, aminoacyl−tRNA biosynthesis, and inositol phosphate metabolism were reported to be changed in the early stage of BC.[15] Herein, we evaluated the plasma metabolomics of BC patients and HC individuals within the UAE population to identify UAE BC-associated changes in metabolites and metabolic pathways and to identify the metabolic signature for possible diagnosis and potential target therapy.

2. METHODS

2.1. Study Subjects

A cohort of 35 patients diagnosed with primary invasive BC at the Sharjah Breast Care Centre (University Hospital Sharjah, Sharjah, UAE) was enrolled in this study. Patients with metabolic disorders were excluded from the study. A total of 30 healthy volunteers were used as the HC. HC individuals were in the age- and sex-matched ranges of the BC cohort. Individuals with obesity (BMI $\geq$ 30 kg/m^2), metabolic syndrome, diabetes mellitus, or other chronic diseases were excluded. Blood samples were obtained from the patients and HC individuals, and the plasma was separated and used for metabolite profiling. This research was conducted in compliance with the Helsinki Declaration guidelines and received approval from the University Hospital Sharjah Ethical and Research Committee (UHS-REC) (Approval Number: UHS- REC-22-05-24-S). Written informed consent was obtained from all patients prior to their enrollment in the study.

2.2. Metabolite Extraction and Analysis Using LC/MS−MS

To identify differentially abundant metabolites (DAMs) between BC patients and HC individuals, blood samples from 35 BC patients and 30 HC individuals were collected in EDTA tubes and centrifuged at 3200 rpm for 15 min at 4 °C. The plasma was collected and stored at −80 °C. For metabolite extraction, 100 μL of plasma was mixed with 300 μL of methanol. The samples were incubated for 10 min, vortexed, and centrifuged at 15,000 rpm at 4 °C. The supernatants were collected and evaporated using a speed vac (Genevac EZ-2 plus, Ipswich, UK). Dried samples were dissolved in 200 μL of 0.1% formic acid and analyzed using LC−MS/MS.

2.3. Protein Extraction and Analysis Using LC/MS−MS

To extract the proteins, 4 μL of the plasma was added to 100 μL of lysis buffer containing 1X protease inhibitors and incubated for 10 min at room temperature. The sample lysates were sonicated and centrifuged at 15,000 rpm at 4 °C for 5 min. The supernatants were collected, and protein precipitation was conducted by the addition of methanol and chloroform. The samples were mixed thoroughly and centrifuged at 13,000 rpm at 4 °C for 5 min. The upper aqueous phase was removed, and the lower phase together with the white protein pellet was resuspended in 300 μL of methanol. The mixture was then centrifuged at 13,000 rpm for 1 min at 4 °C, after which the supernatants were discarded. The protein pellets were further air-dried, resuspended in denaturation solution, and quantified using the Bradford assay.

Proteomics analysis using LC−MS/MS was conducted to identify the differentially expressed proteins (DEPs) between BC patients and HC individuals; protein samples were prepared by using in-solution digestion. In brief, 10 μL of 10 mM dithiothreitol (DTT) (final concentration of 1 mM) was used to reduce 100 μg of denaturated protein. The samples were then alkylated with 10 μL of 55 mM iodoacetamide (IAA) (final concentration 5.5 mM) and incubated for 1 h at room temperature at 100 rpm in the dark. The pH was adjusted to 8.0 in all reactions. Protein digestion was performed using 1 μg of Lysyl Endopeptidase LysC (1:100 ratio), and this was followed by dilution in 4 volumes of 20 mM ammonium bicarbonate and digestion with trypsin (1:100 ratio) overnight. In the next day, the samples were dried using EZ-2 Plus (GeneVac-Ipswich, UK) and resuspended with 100 μL of 1% trifluoroacetic acid (TFA). Peptides were then desalted using Pierce C18 stage tips (Thermo Scientific, Waltham, USA). After repeatedly aspirating and dispensing 100 μL of 50% acetonitrile (ACN) to activate Pierce C 18 tips, 100 μL of 0.1% TFA was used to equilibrate the tips. Sample peptides were then loaded by repeatedly aspirating and dispensing the sample volume 10 times. Similar procedures were used to wash the peptides with 5% ACN and 0.1% TFA. They were then eluted by gently aspirating and repeatedly dispensing 100 μL of 60% ACN and 0.1% formic acid (FA) 10 times. Prior to being analyzed by LC−MS/MS, desalted peptides were dried in EZ-2 Plus and reconstituted in 0.1% FA and 2% ACN.

2.4. High-Performance Liquid Chromatography Tandem Mass Spectrometry (HPLC−MS/MS) for Metabolite Analysis

Metabolites were separated and detected using an Elute UHPLC and a QTOF-MS system with a Hamilton Intensity Solo C18 column (100 mm × 2.1 mm, 1.8 μm beads) (Bruker Daltonik). Solvents A (0.1% FA in HPLC-grade water) and B (0.1% FA in ACN) were used for inline reversed-phase chromatography (Bruker, Bremen, Germany). An Apollo II electrospray ionization (ESI) source was employed for analysis. The column was kept at 35 °C for metabolomics analysis. Metabolite extracts were injected, eluted, and re-equilibrated using 1% ACN at flow rates of 250 and 350 μL/min for elution and re-equilibration, respectively, throughout a 30 min gradient of 1% to 99% ACN. The drying gas was set at 10 μL/min, drying temperature at 220 °C, and nebulizer pressure at 2.2 bar. In auto-MS/MS mode, the scan ranges were 50−1300 m/z. The collision energy was 20 eV with a 0.5 s cycle.

To ensure the analytical reliability and reproducibility of metabolomics data sets, stringent validation and quality-control (QC) procedures were implemented throughout the experimental workflow. Bruker T-ReX LC-QTOF solution was used to assess the mass spectrometer and column performance. For the Bruker T-ReX LC-QTOF solution, which was supplied by Nova Medical Testing Inc., TRX-3112-R/MS certified human serum was used for the reversed-phase liquid chromatography (RPLC) separation and multipoint retention time calibration. Prior to sample analysis, all LC−MS instruments were calibrated using manufacturer-recommended standard tuning solutions to achieve mass accuracy < 5 ppm and retention time deviation < 0.2 min. Sample injection order was randomized to minimize systematic bias. Pooled QC samples, prepared by combining 10 μL of all biological samples, were analyzed at the beginning of the sequence to assess the column conditions and subsequently after every 10 injections to monitor instrument stability and analytical drift. Metabolites with a relative standard deviation (RSD) >30% in QC samples were excluded from downstream analysis. The reproducibility of QC samples was confirmed by tight clustering in PCA plots. Blank samples were interspersed to assess carry-over and background contamination.

External mass calibration (10 mM sodium formate calibration solution) was used to accomplish mass calibration prior to analysis, and the mixture was injected at the beginning of each sample run and used for internal calibration during data processing.

https://doi.org/10.1021/acs.jproteome.5c00669
J. Proteome Res. XXXX, XXX, XXX−XXX

2.5. HPLC−MS/MS for Peptide Analysis

For peptides, a nano elute (Bruker Daltonics) coupled to a quadrupole-time-of-flight mass spectrometer (QTOF) was utilized to perform the LC−MS/MS analysis (Bruker Daltonics) with a Captive Spray ion source (Bruker Daltonics). An amount of the sample measuring 4 μL (4 μg of the peptides) was injected and trapped using an Acclaim PepMap C18 (5 mm, 300 μm id, 5 μm particle diameter, 100 Å pore size) trap cartridge (Thermo Fisher Scientific), and the separation was performed on a FIFTEEN column C18 15 cm × 75 um, 1.9 um (Bruker). Peptide separation was carried out over a 140 min gradient as follows: 0 to 5 min, 5% B; 5 to 120 min, 5−35% B; 120 to 125 min, 35−95% B; 125 to 135 min, 95% B; 135 to 135.2 min, 95−5% B; 135.2−140, 5% B. The flow rate was 0.30 μL/min. The Captive Spray ion source conditions for every injection were as follows: the drying gas flow rate was 3.0 L/min at a temperature of 150 °C, and the capillary voltage was set at 1600 V. In the auto-MS/MS mode, the scan ranges were 150−2200 m/z. The collision energies varied from 23 to 65 eV with a 3 s cycle.

To monitor system performance and ensure analytical consistency, a Pierce HeLa Protein Digest Standard (Thermo Fisher Scientific, Waltham, Massachusetts, USA) was injected prior to each sample. The HeLa digest served as a QC reference to assess the mass accuracy, chromatographic stability, and reproducibility of peptide identification and retention times throughout the analytical batch. External mass calibration (10 mM sodium formate calibration solution) was used to accomplish mass calibration prior to analysis.

2.6. Metabolomics Data Processing and Analysis

MetaboScape 4.0 software (Bruker, Bremen, Germany) was used to process the data. Molecular feature detection in the T-ReX 2D/3D workflow was optimized using peak duration limitations and an intensity threshold. Only characteristics found in at least six samples were retained after mass recalibration to a retention time range of 0−0.3 min. The MS/MS import method was configured for averaging. Bucketing parameters were established with a mass range of 50 to 1300 m/z and a retention time range of 0.3 to 25 min. MS/MS spectra and retention time (RT) were used to accurately identify unknown chemicals in the QTOF- MS data. To identify metabolites, the Human Metabolome Database (HMDB) 4.0 was utilized. The MS/MS spectra and RT were used as a reference for final compound selections. In cases where several features corresponded to the same database entry, the entry with the highest annotation quality (AQ) score was chosen for each metabolite. The selection method was based on RT, tandem MS/MS data, mass-to-charge (m/z) ratio, analyte lists, mSigma values, and spectral library matching. All samples were prepared and analyzed under identical extraction and injection conditions; therefore, sample normalization was dependent on using same parameters and time and injection of reference solution. Likewise, data transformation was not applied because the distribution of peak intensities did not show significant skewness after feature filtering. To ensure comparability and equal contribution of all variables in multivariate analysis, autoscaling (mean-centering and division by standard deviation) was applied in MetaboAnalyst 5.0. The analytical stability was verified by tight QC sample clustering in PCA and by excluding metabolites with relative standard deviation (RSD) > 30% across QC samples. For multivariate analysis, autoscaling was applied to the metabolomics data set to ensure comparability and variance normalization across metabolites.

To identify the DAMs between BC patients and HC individuals, several univariate and multivariate analyses were performed using the MetaboAnalyst 5.0 platform (https://www.metaboanalyst.ca).[16] Student's t test was employed to compare between the groups. Orthogonal Partial Least Squares Discriminant Analysis (OPLS-DA) was used as a supervised multivariate statistical approach to determine and discriminate the variation in the predictor variables that is informative for class discrimination and orthogonal to the response. In the current work, OPLS-DA was utilized to form group discrimination models and determine the informative features that impact classification performance. Hierarchical clustering analysis (HCA) was performed to visualize the metabolomics grouping resulting from the difference between metabolites extracted from BC patients and HC individuals. The false discovery rate (FDR) was used to eliminate false positives and correct for multiple hypothesis testing. Metabolites with q-value <0.05 were considered significant.

Univariate analyses were conducted to calculate the area under the receiver operating characteristic curve (AUROC), false discovery rate (FDR)-adjusted q-values, and fold changes (BC/HC) for each candidate marker. Recognizing the potential for inflated model performance and the critical role of accurate predictions in clinical applications, we rigorously validated the model using a 100-permutation test for internal validation. The model's explanatory and predictive capabilities were assessed using R^2 and Q^2 metrics, respectively.

Metabolite set enrichment analysis (MSEA) were also performed using MetaboAnalyst to interpret the metabolic differences between the tested groups. MSEA identifies biologically meaningful patterns from significant metabolites (q-value <0.05) by testing their enrichment in curated metabolite sets.

2.7. Proteomics Data Processing and Analysis

The protein and peptide identification was performed using the *Homo sapiens* Uniprot proteome and the Andromeda search engine, and the raw data were processed using MaxQuant version 1.6.17.0 (https://www.maxquant.org/).[17,18] Methionine oxidation and N-terminal acetylation were set as the variable modifications, and carbamidomethylation of cysteine residues was set as the fixed modification. Protein group identification involved the requirement of one minimum unique peptide per protein and two peptides in total. The default settings were kept for all other parameters. The FDR of 1% was set on peptide-spectrum matches (PSMs) and protein group identifications. The precursor mass tolerance for PSMs was set at 20 ppm. Label-free quantification (LFQ) was executed using the MaxLFQ algorithm, and the in silico digestion was performed according to the standard rule of trypsin/P cleavage.[17,19]

Perseus software (2.0.5.0) was utilized for data processing.[20] Proteins that were found to be potential contaminants, reversed sequences, and those only based on site localization were eliminated from the data set. The values of LFQ generated by MaxQuant were log2-transformed and normalized to mitigate systematic variation across the samples. Multiple normalization strategies were systematically evaluated. Global median centering was applied by subtracting the sample-specific median $\log_2$ intensity across all quantified features, correcting for global shifts in signal intensity. The aim of median normalization is to center the data to the median of distribution of each sample.[21] Quantile normalization was applied to enforce consistent intensity distributions across samples, which helps minimize distributional differences but may modify the covariance structure. Z-score normalization was applied by centering and scaling features to zero mean and unit variance, primarily for visualization purposes.[22,23] In addition, a subset-based normalization approach using empirically invariant features was implemented. Proteins exhibiting low variability across samples (coefficient of variation (CV) < 10% (CV)) were identified from unnormalized log2-transformed data, and the top 10 most stable proteins were used to drive sample-specific normalization factors (CV-low subset normalization).[23,24] Housekeeping subset normalization using 61 selected stable plasma proteins (complement components, coagulation factors, and transporters) was also evaluated; however, instability of several candidate reference proteins limits their suitability for primary normalization. Normalization performance was assessed using boxplots of sample intensity distributions and principal component analysis (PCA) to evaluate variance structure and potential normalization-induced distortion.

Annotated proteins were trimmed to include only the proteins with at least 70% valid values. Missing values were then separately imputed for every sample by using the normal distribution with the downshift of 1.8 and the width of 0.3. Proteins with notable expression alterations in BC patients were confirmed using the two-tailed independent Student's t test. The Benjamini−Hochberg procedure was performed to account for the number of comparisons. Proteins were deemed differentially expressed when the FC threshold is 1.5 and q-value <0.05. Hierarchical group expression profiles were compared using the hierarchical

https://doi.org/10.1021/acs.jproteome.5c00669
J. Proteome Res. XXXX, XXX, XXX−XXX

clustering, and the resultant patterns were visualized in the form of the heatmap. All figures were prepared using the R software. Gene ontology was conducted using string (https://www.string-db.org/).

2.8. Integrated Metabolomics and Proteomics Analysis

To identify functionally related metabolites and proteins, joint-pathway analysis for DAMs and DEPs between BC patients and HC individuals was performed using the Metaboanalyst 5.0 software network analysis tool. The common significant pathways among all combined features of metabolites and proteins listed in BC patients versus HC individuals were identified using rigorous integration through combined queries, topological analysis using the degree centrality method, and enrichment analysis via hypergeometric testing ($P < 0.05$). The direct and indirect relationships between the DAMs and DEPs were conducted using Stitch (http://stitch.embl.de/), Cytoscape version 3.10., and cytoHubba to generate and analyze the interaction network.

3. RESULTS

3.1. Clinicopathological Characteristics of BC Patients

A cohort of 35 BC patients and 30 HC individuals were involved in this study. The clinicopathological characteristics of BC patients are shown in Table 1.

Table 1. Clinicopathological Characteristics of BC Patients[a]

parameters			total no. of samples = 35
diagnosis: *n* (%) [*N* = 31]	IDC		28 (90.3%)
	ILC		2 (6.5%)
	mixed		1 (3.2%)
molecular subtype: *n* (%) [*N* = 32]	luminal a & luminal B HER-2 negative	luminal	24 (75%)
	luminal B HER-2 positive	triple positive	5 (15.6%)
	triple negative	triple negative	3 (9.4%)
stage: *n* (%) [*N* = 30]	stage 0&1	early stage	18 (60%)
	stage 2		
	stage 3	late stage	12 (40%)
	stage 4		

[a]Note: IDC; invasive ductal carcinoma, ILC; invasive lobular carcinoma.

In our cohort, 90.3% of patients were diagnosed with invasive ductal carcinoma (IDC), 6.5% with invasive lobular carcinoma (ILC), and 3.2% with a mixed phenotype. According to the molecular subtype, BC patients were classified based on the expression of estrogen receptor (ER), progesterone receptor (PR), and HER-2 into luminal subtypes including patients with luminal A (ER+/PR+/HER-2−) and luminal B (ER+/PR+/HER-2−), triple positive patients including patients with luminal B HER-2 positive patients' subtype (ER+/PR+/HER-2+) and triple-negative patients (ER+/PR+/HER-2−). Luminal subtypes encompass 24 (75%), triple positive constitutes 5 patients (15.6%), and triple-negative is represented by only 3 patients (9.4%) (Table 1). The HER-2 positive group was separated as HER-2 overexpression represents a biologically and clinically distinct phenotype, often associated with a higher tumor grade, increased proliferation, and specific therapeutic implications (e.g., trastuzumab-based therapy). In addition, HER-2 positive tumors were predominant in younger females in the UAE.[7] 18 Patients (60%) were in the early stages [stage 0 (1 patient), stage 1 (8 patients), and stage 2 (9 patients)], while 12 patients (40%) were in the late stages [stage 3 (9 patients) and stage 4 (3 patients)]. Most patients were positive for ER (90.6%), and only 3 patients (9.4%) were negative for ER (Table 2). Similarly, most of the patients (87.5%) were positive for PR and only 4 patients (12.5%) were negative. HER-2 was negatively observed in 24 patients (80%). The proliferation marker K_i-67 was positive in 21 patients (67.7%) and negative in 10 patients (32.3%; Table 2).

Table 2. Histopathological Characteristics of BC Patients[a]

variables		total no. of samples = 35
ER: *n* (%) [*N* = 32]	negative	3 (9.4%)
	positive	29 (90.6%)
PR: *n* (%) [*N* = 32]	negative	4 (12.5%)
	positive	28 (87.5%)
HER-2: *n* (%) [*N* = 33]	negative	27 (81.8%)
	positive	6 (18.2%)
K_i67: *n* (%) [*N* = 31]	negative (<14%)	10 (32.3%)
	positive (>14%)	21 (67.7%)

[a]Note: One HER-2 positive patient had missing ER and PR data and was therefore not included in the molecular subtype classification.

Collectively, out of 35 BC patients, a predominance of the luminal subtype was detected with a significant proportion in early-stage disease and high positivity rates for ER, PR, and K_i-67. The majority exhibits HER-2 negativity, highlighting distinct clinical−pathological profiles that may guide targeted therapeutic strategies.

Among the studied cohort, 19 patients (61.3%) received hormone therapy, 7 patients (22.6%) were treated with targeted therapies (including anti-HER-2 agents and CDK4/6 inhibitors), 3 patients (9.7%) underwent chemotherapy, and 2 patients (6.5%) received surgical treatment.

3.2. Metabolomics Analysis Showed Significant Differences in Metabolic Profiles between BC Patients and HC Individuals

Metabolomics analysis was conducted to identify DAMs in BC patients compared to HC individuals. A total of 135 metabolites were detected using LC/MS−MS, of which 16 were significantly different between the two groups (q-value <0.05). Notably, 4 metabolites including hypoxanthine, allantoic acid, 2-phenylbutyric acid, and uridine were significantly upregulated in BC patients (FC > 1.5, q-value <0.05). However, 12 metabolites including vitamin D3, *N*-acetylputrescine, 9-methyluric acid, thyroxine, indoleacetic acid, guanidine, L-arginine, guanidinosuccinic acid, androstenedione, L-homocysteic acid, urocanic acid, and PC (18:1(9Z)/18:1(9Z)) were significantly downregulated in BC patients relative to HC (FC = 0.2−0.6, q-value <0.05) (Figure 1A and Table 3).

To examine the overall metabolic difference between BC patients and HC individuals, HCA analysis was performed (Figure 1B). HCA classified the metabolite profiles into two distinct clusters: one characterized by metabolites showing peak abundance in BC patients, while the second cluster included metabolites enriched in the HC group (Figure 1B).

Further analysis was conducted to identify specific biomarkers between early- and late-stage BC. Only in early BC patients, L-arginine, guanidine, isocitric acid, guanidinosuccinic acid, indoleacetic acid, ethanolamine, diethanolamine, and thyroxine levels were significantly (q-value <0.05) downregulated, while hypoxanthine was significantly upregulated compared to the HC group, reflecting altered metabolic pathways critical to early tumor development particularly those involved in amino acid and energy metabolism (Table 4, Figures S1, and S2). Figures S1

https://doi.org/10.1021/acs.jproteome.5c00669
J. Proteome Res. XXXX, XXX, XXX−XXX

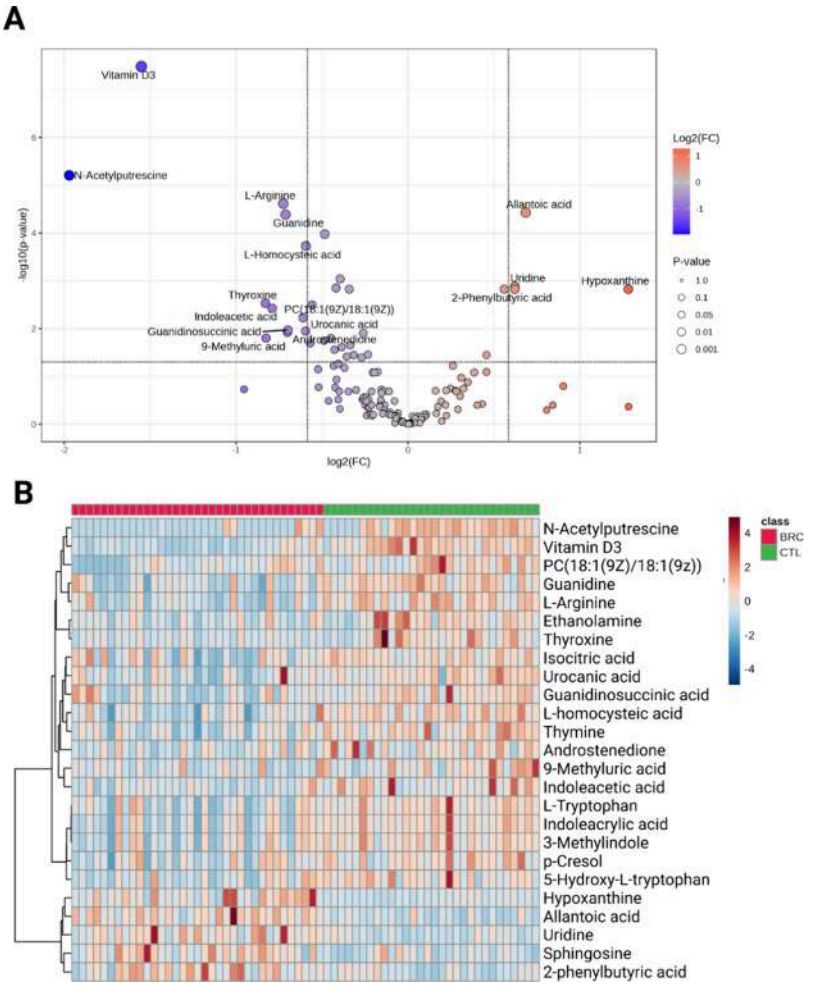

Figure 1. Metabolomics profiling demonstrates significant differences in metabolites between breast cancer (BC) patients and healthy controls (HC). (A) Volcano plot for differentially abundant metabolites (DAMs) between BC and HC groups that have a fold change threshold of 1.5 and q-value <0.05. The red color indicates the upregulated metabolites, while the blue color indicates downregulated metabolites. (B) Hierarchical clustering analysis (HCA) of metabolites that were significantly (q-value <0.05) different between the two populations. The heatmap displays the relative abundance levels of significant metabolites, with each row representing an individual metabolite and each column corresponding to a biological replicate. Gradients from red through blue reflect relative metabolite levels. Red color indicates a high level, while blue color indicates a low level. BRC; breast cancer patients, CTL; healthy control.

and S2 present boxplots showing the relative abundance of significant metabolites across control, early-, and late-stage BC groups, emphasizing the clear alteration in amino acid-related metabolites in early-stage patients. In late-stage BC, pipecolic acid and estradiol were found to be significantly (q-value <0.05) increased only in patients with late-stage BC compared to HC, indicating an enhanced lysine degradation and hormonal dysregulation.[25,26] However, PC (18:1(9Z)/18:1(9Z)), urea, and androstenedione were significantly (q-value <0.05) reduced in late BC patients compared to the HC group, indicating metabolic reprogramming that favors tumor progression (Table 4, Figures S1, and S2). Allantoic acid was significantly upregulated in both early- and late-stage BC. Vitamin D3, *N*-acetylputrescine, urocanic acid, and L-homocysteic acid were significantly downregulated in both early- and late-stage BC.

Furthermore, a significant increase (FC = 4.75, q-value <0.05) in biotin levels was observed in patients with a high proliferative tumor (K_i-67 > 14%) compared to patients with low proliferative (K_i-67 < 14%), indicating that this metabolite is important for cancer cell proliferation and further investigations are warranted to identify its role in BC cell proliferation. All of these alterations indicate that the tumor is in increased demand for specific metabolites to support rapid proliferation and survival, highlighting potential opportunity for biomarker development and therapeutic intervention.

Collectively, the metabolomics analysis revealed significant metabolic alterations between BC patients and HC individuals with distinct upregulation and downregulation of key metabolites linked to tumor progression, proliferation, and stage-specific metabolic reprogramming. The main metabolic pathway altered in BC patients is amino acid metabolism, particularly arginine metabolism, tryptophan metabolism, and lysine metabolism. These pathways are critical for providing biosynthetic precursors, supporting energy demands, and facilitating tumor proliferation and progression, making them potential targets for biomarker development and therapeutic intervention.

3.3. Identification of Biomarkers and Analysis of Model Performance

OPLS-DA was employed to determine group separation and key metabolites responsible for classification in a pairwise comparison. To validate the model reliability, 100-permutation

https://doi.org/10.1021/acs.jproteome.5c00669
J. Proteome Res. XXXX, XXX, XXX−XXX

Table 3. Significantly Downregulated and Upregulated Metabolites between BC and HC (FC Cutoff 1.5 and *q*-Value <0.05)

metabolites	AUROC	VIP score	FC (BC/HC)	FDR *q*-value
vitamin D3	0.92	2.4	0.34	3.28×10^{-08}
N-acetylputrescine	0.82	2.48	0.26	6.21×10^{-06}
L-homocysteic acid	0.83	1.86	0.66	1.88×10^{-04}
guanidine	0.83	2.22	0.61	4.11×10^{-05}
L-arginine	0.84	2.16	0.61	2.43×10^{-05}
allantoic acid	0.87	2.04	1.61	3.73×10^{-05}
hypoxanthine	0.77	1.55	2.43	1.50×10^{-03}
uridine	0.81	2.01	1.54	1.31×10^{-03}
2-phenylbutyric acid	0.75	1.68	1.54	1.50×10^{-03}
PC (18:1(9Z)/18:1(9Z))	0.71	1.51	0.66	5.94×10^{-03}
9-methyluric acid	0.73	1.39	0.56	1.58×10^{-02}
thyroxine	0.76	1.67	0.56	2.96×10^{-03}
indoleacetic acid	0.76	0.97	0.58	3.76×10^{-03}
androstenedione	0.71	1.1	0.61	1.20×10^{-02}
guanidinosuccinic acid	0.74	1.42	0.62	1.07×10^{-02}
urocanic acid	0.80	1.36	0.66	1.13×10^{-02}

Table 4. Significantly Downregulated and Upregulated Metabolites in Early BC Compared to HC (FC Cutoff 1.5 and *q*-Value <0.05) and Late BC Compared to HC

	early BC		late BC	
metabolites	FC (EBC/HC)	*q*-value	FC (LBC/HC)	*q*-value
L-arginine	0.51	1.47×10^{-05}		
guanidine	0.52	1.47×10^{-05}		
isocitric acid	0.66	3.23×10^{-03}		
guanidinosuccinic acid	0.50	3.21×10^{-03}		
indoleacetic acid	0.49	9.50×10^{-03}		
ethanolamine	0.65	1.69×10^{-02}		
diethanolamine	0.60	2.23×10^{-02}		
thyroxine	0.55	2.91×10^{-02}		
hypoxanthine	2.26	3.21×10^{-03}		
allantoic acid	1.59	1.50×10^{-05}	1.53	1.01×10^{-03}
N-acetylputrescine	0.27	4.91×10^{-04}	0.26	4.26×10^{-03}
urocanic acid	0.55	6.15×10^{-04}	0.62	2.01×10^{-02}
L-homocysteic acid	0.65	2.27×10^{-03}	0.63	4.26×10^{-03}
vitamin D3	0.35	1.50×10^{-05}	0.32	1.01×10^{-03}
pipecolic acid			1.53	2.72×10^{-03}
PC (18:1(9Z)/18:1(9Z))			0.48	6.34×10^{-03}
urea			0.55	5.45×10^{-03}
estradiol			1.65	1.75×10^{-02}
androstenedione			0.49	3.87×10^{-02}

tests were conducted. The findings showed good separation between the BC and HC groups (PC1 = 8.6%, PC2 = 15.4%) (Figure 2A). The model showed good values of explained ability (R2) and predictive ability (Q2) (R2Y = 0.829, $P < 0.01$ and Q2 = 0.708, $P < 0.01$) (Figure 2B). A total of 49 key metabolites were identified from the OPLS-DA model having a VIP score ≥ 1. Among the top 15 metabolites identified were *N*-acetylputrescine, vitamin D3, guanidine, L-arginine, L-homocysteic acid, indoleacrylic acid, thymine, 3-methylindole, L-tryptophan, ethanolamine, and thyroxine, which were high in the HC group. Increased levels of allantoic acid, uridine, sphingosine, and 2-phenylbutyric acid were observed in BC subjects (Figure 2C).

For selection of biomarkers that could be used in BC diagnosis, univariate ROC analysis of DAMs was conducted. Metabolites with AUROC > 0.7 were selected as potential biomarkers. Using the whole data set, the model was 0.954 in AUROC (95% CI: 0.843−0.998), indicating high sensitivity and specificity (Figure 2D). These results indicate that BC patients could be distinguished from HC by specific metabolic signatures (Figure 2E).

Based on a VIP score ≥ 1.5, an FC threshold of 1.5, and a *q*-value <0.05, 11 metabolites were selected as potential biomarkers for diagnosis of BC (Figure 3 and Table 3).

To evaluate the potential confounding effect of treatment heterogeneity, breast cancer samples were stratified into endocrine-based therapy (hormone therapy ± CDK4/6 inhibitors) and other treatment modalities. PCA revealed a substantial overlap between treatment groups, indicating that treatment exposure does not dominate the global metabolic variance structure (Figure S3). Consistent with PCA results, hierarchical clustering of stage-associated metabolites showed no distinct treatment-driven clusters, further supporting the idea that treatment status does not account for the major molecular patterns observed.

3.4. Metabolite and Structural Motifs of Early- and Late-Stage BC in Representative UAE Population

To map the biochemical and structural signatures underlying BC progression, we analyzed stage-specific metabolite-level pathway motifs and structural chemical features that distinguish early from late-stage disease. In early-stage BC, the metabolomic pattern is predominantly enriched with small, polar molecules characterized by guanidino (−N═C(N)N) or amino acid-derived functional groups such as L-arginine, guanidine, and guanidinosuccinic acid, as well as short-chain polar moieties (e.g., ethanolamine, diethanolamine) and multicarboxylates like isocitric acid. These structural motifs point to a reliance on nitrogen metabolism, urea cycle intermediates, and early oxidative phosphorylation demands, reflecting an initial cellular adaptation to proliferative stress. In contrast, late-stage BC exhibits a metabolomic profile dominated by larger, lipophilic compounds featuring steroidal backbones (e.g., estradiol androstenedione), aromatic heterocycles (e.g., uric acid derivatives), complex phospholipids such as PC(18:1/18:1), and various amide-containing metabolites. This transition from small, hydrophilic to complex, hydrophobic chemical architectures suggest a significant biochemical evolution of the tumor microenvironment, from early-stage reliance on amino acid and energy metabolism to late-stage dependence on lipid remodeling, hormonal dysregulation, and membrane biogenesis. Structural motif analysis, therefore, revealed a distinct trend in metabolic evolution: a progressive shift from amino acid-like and polar metabolite signatures in early stages to steroidal, lipid-rich, and membrane-associated signatures in advanced disease. This progression reflects a metabolic rewiring that aligns with known hallmarks of cancer, including sustained proliferation, immune evasion, and endocrine resistance. These findings support the potential utility of structural motif profiling as a diagnostic and staging tool while also identifying novel targets for stage-specific therapeutic intervention.

https://doi.org/10.1021/acs.jproteome.5c00669
J. Proteome Res. XXXX, XXX, XXX−XXX

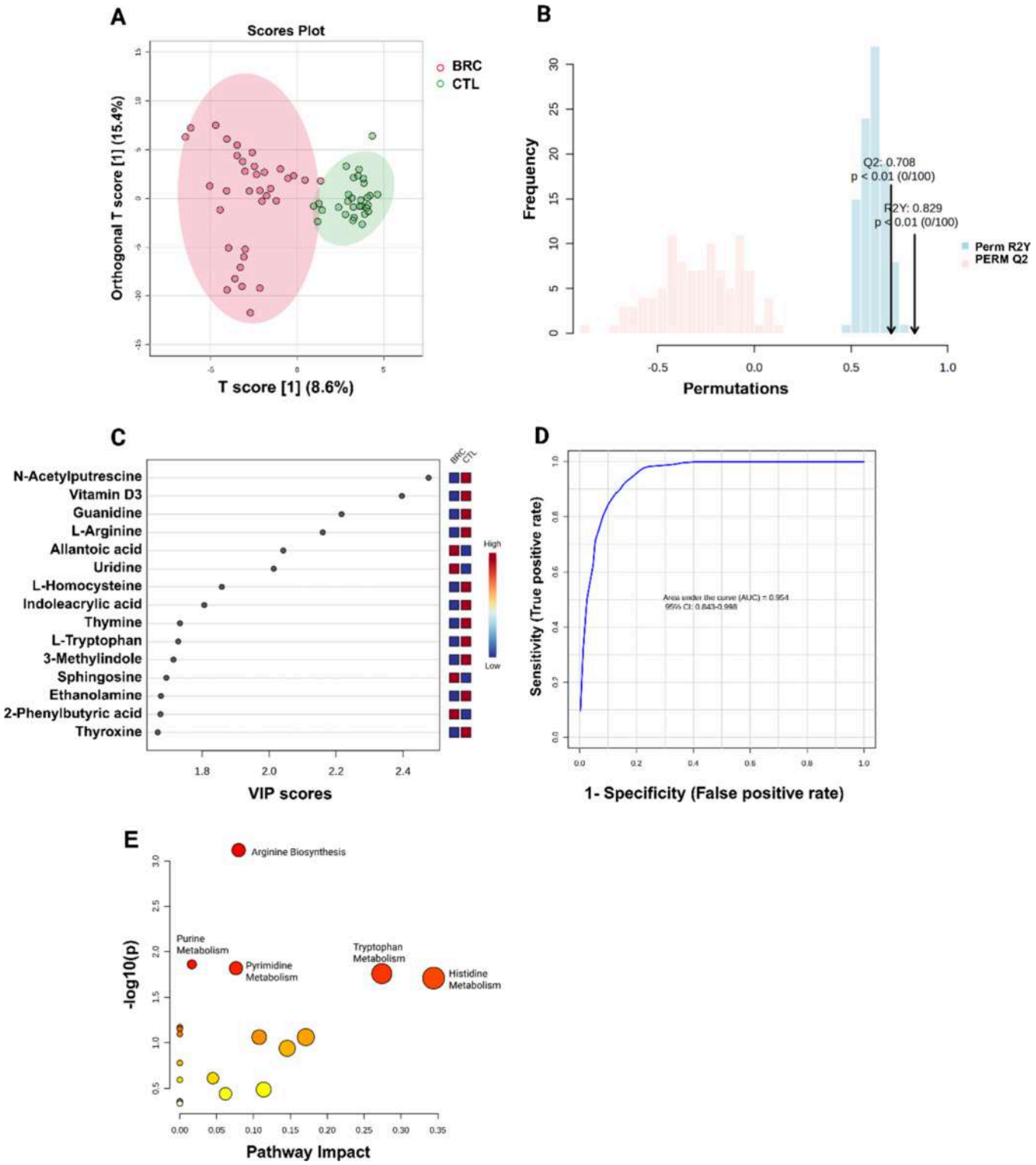

Figure 2. Model development and validation for BC diagnosis. (A) Score plots from the OPLS-DA model showing the separation between the BC and HC groups. Each point represents an individual sample: red for breast cancer patients, green for healthy control. (B) Permutation testing of the OPLS-DA model ($n = 100$). (C) Important metabolites recognized by the variable importance in projection (VIP) score obtained from the OPLS-DA model. (D) ROC curve of the prediction efficacy for the metabolites obtained from the OPLS-DA model. (E) Pathway analysis based on metabolic enrichment analysis.

3.5. Significant Alteration in Metabolic Pathways in BC Patients

MSEA was performed to identify the significant metabolite pattern (q-value <0.05) between BC patients and HC individuals. The altered metabolic pathways include arginine biosynthesis, purine metabolism, pyrimidine metabolism, tryptophan metabolism, and histidine metabolism (Figure 4), which were previously reported to be linked with cancer development and progression.[27−31]

https://doi.org/10.1021/acs.jproteome.5c00669
J. Proteome Res. XXXX, XXX, XXX−XXX

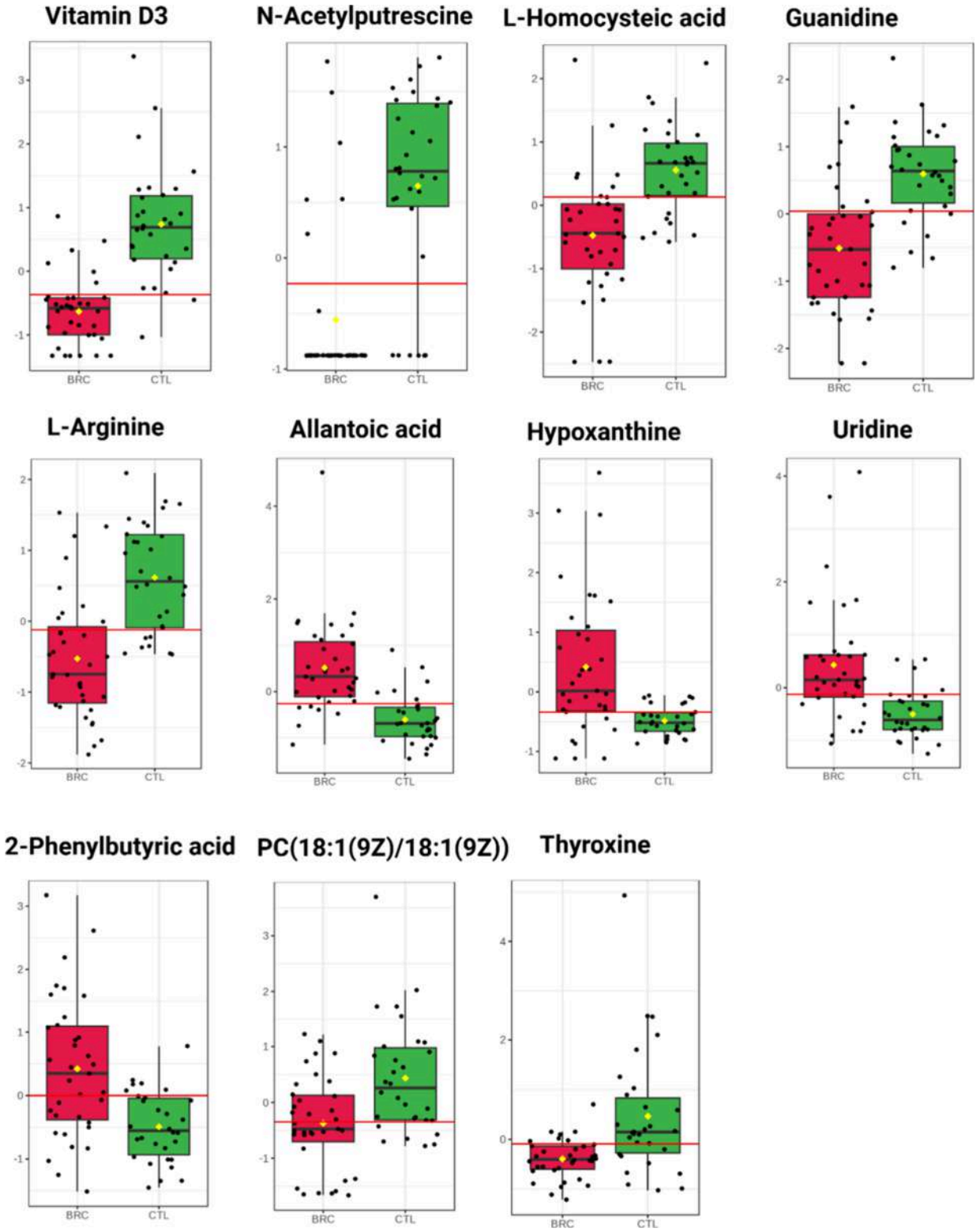

Figure 3. Metabolic signature for BC diagnosis. Differential expression of the final set of metabolites between BC patients and HC individuals that were selected as biomarkers for BC diagnosis.

3.6. Evaluation and Selection of the Normalization Method for Proteomics Analysis

Comparative assessment of normalization strategies demonstrated that global and distribution-based methods (median, quantile, and Z-score normalization) reduced technical variability but introduced varying degrees of variance compression or covariance distortion. In contrast, CV-low subset normalization based on invariant proteins preserved the biologically plausible variance structure while minimizing technical effects. PCA and boxplot comparisons (Figures S4 and S5) indicated that CV-low subset normalization provided the most stable and interpretable data structure, with reduced

https://doi.org/10.1021/acs.jproteome.5c00669
J. Proteome Res. XXXX, XXX, XXX−XXX

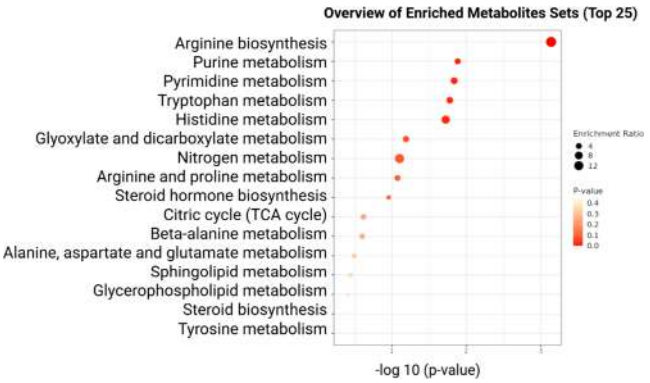

Figure 4. Metabolite set enrichment analysis (MSEA) for significant metabolites (q-value <0.05) between BC patients and HC ranked by the Holm P-value.

technical bias and retention of expected biological heterogeneity. Accordingly, CV-low subset normalization was selected for all subsequent univariate and multivariate analyses, including heatmap visualization, OPLS-DA modeling, permutation testing, and VIP scores.

3.7. Proteomics Analysis Showed Significant Changes in Proteins between BC Patients and HC Individuals

To identify DEPs between BC patients and HC individuals, proteomics analysis was conducted. 166 proteins were detected using LC-MS/MS, and 42 of them were significantly different (q-value <0.05) between BC patients and HC individuals. Five proteins were significantly upregulated (FC > 1.5), while 3 proteins were significantly downregulated (Table 5 and Figure 5A). Hemoglobin subunits were found to be dysregulated. Literature review indicates that hemoglobin abundance in plasma is highly sensitive to preanalytical factors such as variable hemolysis rather than true biological constancy.[32] Therefore, hemoglobin subunits were excluded from the biomarker list.

Table 5. Significantly Downregulated and Upregulated Proteins in BC Patients Compared to the HC Group (FC Cutoff 1.5 and q-Value <0.05)

gene names	protein names	q-value	VIP score	FC(BC/HC)
CD5L	CD5 antigen-like	6.67×10^{-04}	1.86	0.61
IGHV3−7	immunoglobulin heavy variable 3−7	0.00×10^{00}	2.01	0.62
IGHM	immunoglobulin heavy constant mu	0.00×10^{00}	1.77	0.64
FN1	fibronectin	1.75×10^{-02}	1.69	1.53
HSPA8	heat shock cognate 71 kDa protein	1.91×10^{-02}	1.39	2.37
S100-A6	protein S100-A6	1.14×10^{-03}	1.89	2.67
VWF	von Willebrand factor	1.66×10^{-02}	1.63	2.91
ACT	actin, cytoplasmic 1	0.00×10^{00}	2.43	3.24
HSP90AB1	heat shock protein HSP 90-beta	0.00×10^{00}	2.27	4.04

HCA was performed to investigate the protein difference between BC patients and the HC group. It classified the proteins into two major clusters: the first cluster includes the proteins that are highly expressed in BC patients, and the second cluster includes proteins that are highly presented in the HC group (Figure 5B).

To investigate differential proteomic profiles of BC patients compared to the HC group, a model using OPLS-DA was applied. Good group separation was seen for BC and HC groups based on the OPLS-DA score plot, encompassing different proteomic signatures (Figure 6A). The validity of the model was complemented by the results of a 100-permutation test, which provided nonoverlapping Q^2 values and ensured that there was no overfitting present. The model exhibited good discrimination with R^2Y = 0.855, and Q^2 = 0.636, which reflected a strong explanatory and predictive capability (Figure 6B). VIP analysis pinpointed some proteins with VIP scores >1.5 indicative of their contribution toward discrimination between the groups (Figure 6C). These results highlight the potential of these proteins to be biomarkers for BC and indicate the need for further biological validation.

Gene ontology analysis (GO) for the significant proteins (q-value <0.05) between BC patients and HC individuals was performed using String (Figure 6D). Pathway analysis identified dysregulation of several immune-related biological processes for BC patients versus HC, with aberrant activation of inflammatory responses, complement activation, and innate and adaptive immunity pathways, implying a multifaceted reprogramming of immune signaling within the tumor microenvironment (Figure 6D).

3.8. Integrated Proteomics and Metabolomics Analysis Showed Significant Dysregulated Metabolic Pathways Particularly the Arginine Metabolism

Integrated metabolomics and proteomics analysis including the DAMs and DEPs between BC patients and HC individuals showed dysregulation in metabolic pathways, including arginine and proline metabolism, linoleic acid metabolism, alpha-linolenic acid metabolism, arginine biosynthesis, and purine metabolism (Figure 7A). These pathways were previously linked to tumor development and progression.[27,30,31]

The interaction between DAMs and DEPs was created using Stitch (Figure 7B). The results showed that heat shock proteins (HSPs) including HSP90AA1, HSP90AB1, and HSPA8 showed high connectivity (hub nodes), suggesting an important regulatory role. These proteins are known to extensively participate in protein folding, stress response, and proteostasis.[33] The HSPs are closely connected with ER (ER1 and ER2) and actin proteins (ACTG1, ACTA2, and ACTC1), indicating their critical role in hormonal signal transduction and cytoskeletal remodeling. Consistently, estradiol, androstenedione, vitamin D, and thyroxine are all connected with ESR1/2 and actin-related proteins, indicating the well-characterized cross-talk between steroid hormones and cytoskeletal reorganization involving nuclear receptor pathways.[34,35] Steroid hormones are well-established drivers of BC development and progression.[34] Cytoskeletal changes, driven by steroid hormones, are known to play an important role in cell migration, invasion, and metastasis.[36] On the other hand, arginine serves as a primary connecting node among several nitrogen metabolic intermediates including guanidine, guanidinosuccinic acid, urea, hypoxanthine, and allantoic acid. This cluster highlights the pivotal role of arginine in nitrogen metabolism and its potential link with hormonal signaling pathways.

3.9. Potential Metabolic Signature of BC Patients from a Representative UAE Population

The metabolic signature in collected blood from BC patients is characterized by enhanced purine and pyrimidine metabolism (hypoxanthine and uridine), hormonal dysregulation and disrupted thyroid and steroid hormones (estradiol, thyroxine, androstenedione), impaired amino acid metabolism (arginine

https://doi.org/10.1021/acs.jproteome.5c00669
J. Proteome Res. XXXX, XXX, XXX−XXX

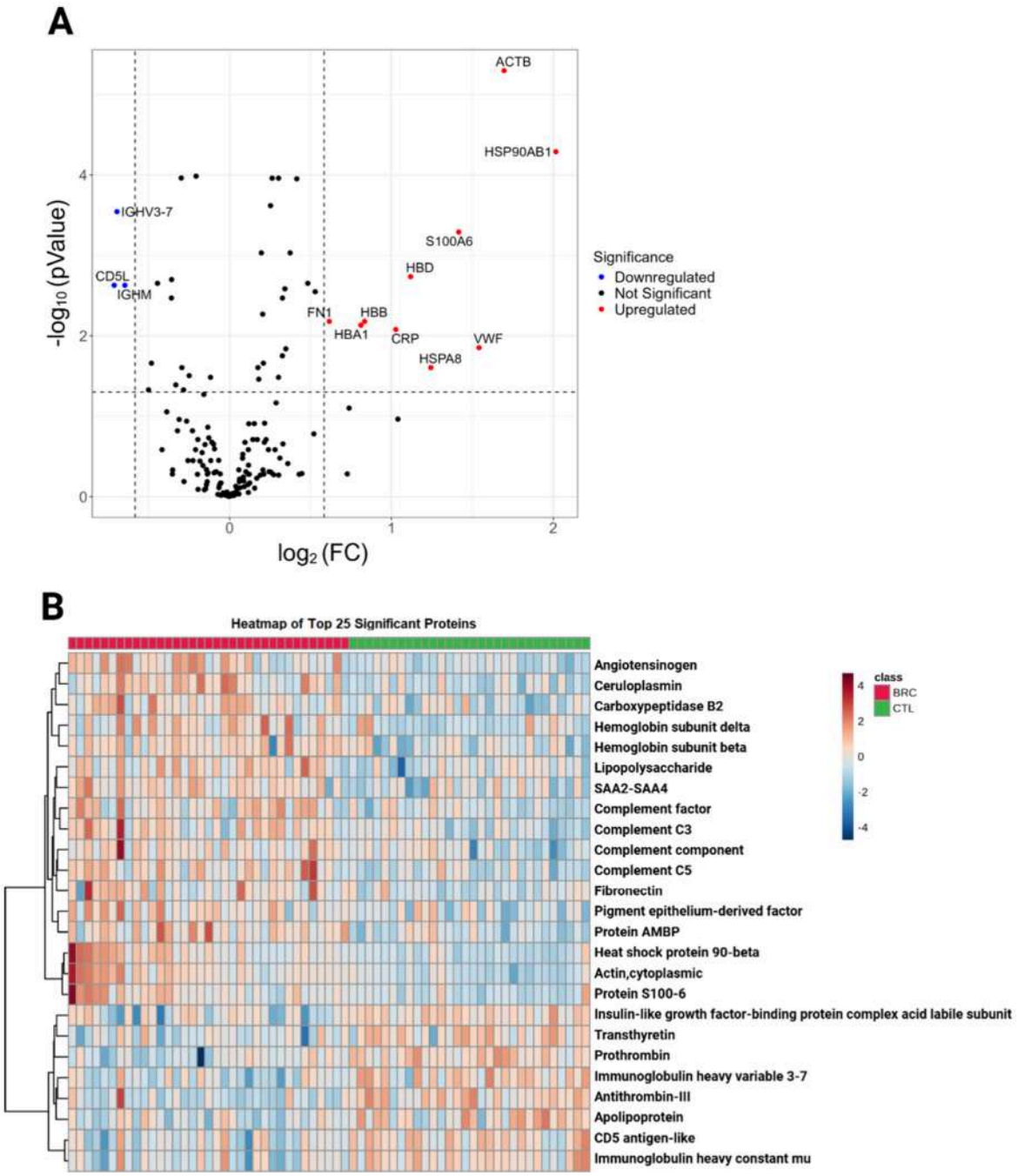

Figure 5. Proteomics profiling demonstrates significant differences in proteins between breast cancer (BC) patients and healthy controls (HC). (A) Volcano plot for differentially expressed proteins (DEPs) between BC and HC groups that have a fold change threshold of 1.5 and q-value <0.05. (B) Hierarchical clustering analysis (HCA) of proteins that were significantly different between the two groups. Gradients from red through blue reflect relative metabolite levels. Red color indicates a high level, while blue color indicates a low level. BRC; breast cancer patients, CTL; healthy control.

and indoleacetic acid), and depletion of immune-modulatory compounds (vitamin D3, arginine). These alterations are strongly implicated as critical metabolic pathways in BC pathogenesis and provide a robust foundation for biomarker discovery and therapeutic targeting.

4. DISCUSSION

BC is the first cause of cancer-related death among females in the Middle East and North Africa (MENA) region, including the UAE.[37] The leading cause of death within these nations is delayed diagnosis and late stage at presentation, leading to a drastic decline in survival rates and narrowed treatment options.[37] Hence, early detection by means of screening is crucial in reducing morbidity and mortality due to BC. Metabolomics, the extensive analysis of small-molecule metabolites in cells, tissues, or biofluids, is a noninvasive strategy for detecting those metabolic alterations. Through analysis of metabolites in blood, urine, or other easily accessible fluids, metabolomics can uncover distinctive metabolic signature marking tumor development, allowing for identifica-

https://doi.org/10.1021/acs.jproteome.5c00669
J. Proteome Res. XXXX, XXX, XXX−XXX

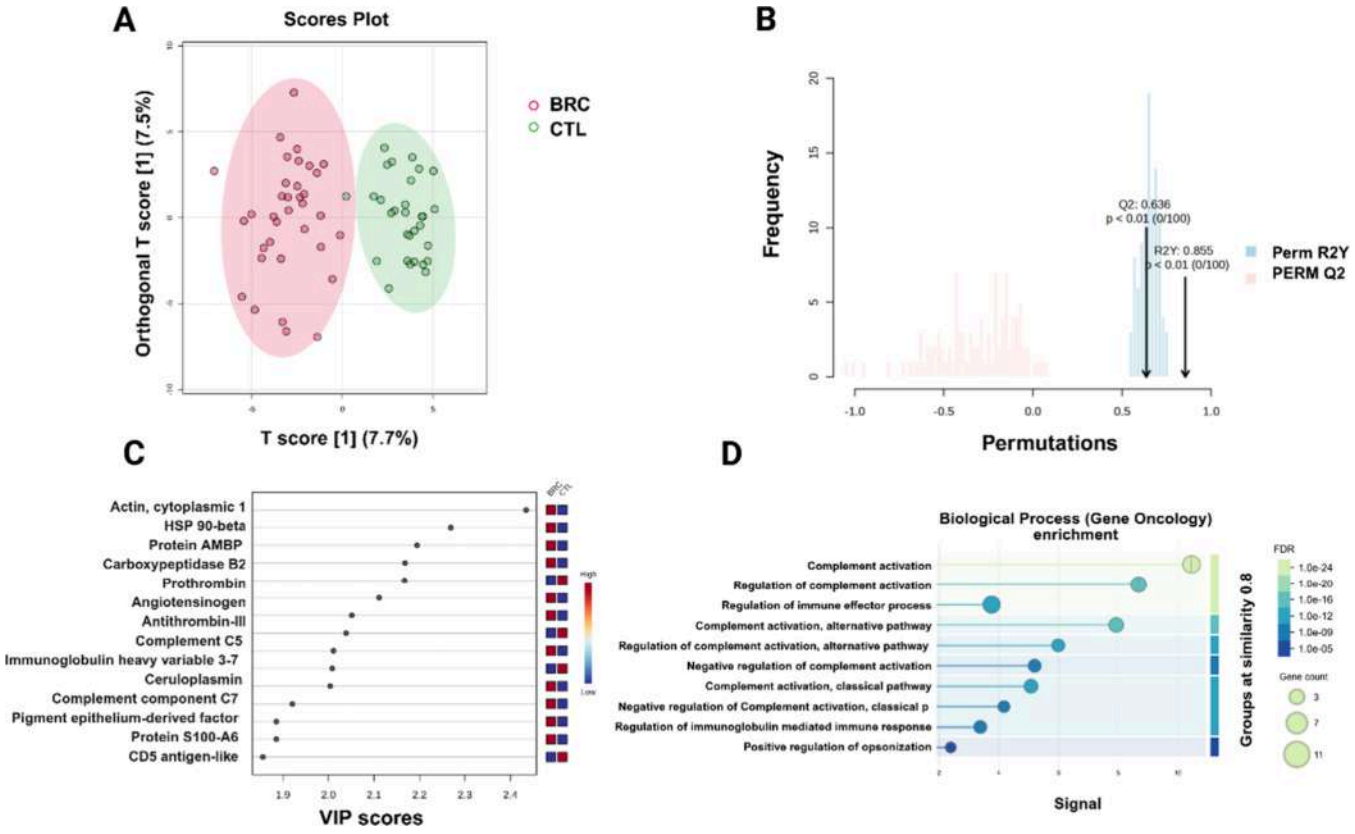

Figure 6. Proteomics signature for BC diagnosis. (A) Score plots from the OPLS-DA model showing the separation between the BC and HC groups. Each point represents an individual sample: red for breast cancer patients and green for the healthy control. (B) Permutation testing of the OPLS-DA model ($n = 100$). (C) Important metabolites recognized by the variable importance in projection (VIP) score obtained from the OPLS-DA model. (D) Gene ontology analysis was obtained using String.

tion of sensitive and specific biomarkers for early detection of cancer.[38] In this study, we conducted metabolomics and proteomics analyses on plasma from 35 BC patients and 30 HC individuals from the UAE population to identify metabolic signature for the diagnosis and targeted therapy of BC. A diagrammatic model illustrating the processes observed from the early stage, the transition phase, to the late stage is presented in Figure 8.

Integrated metabolomics and proteomics analysis identified arginine and proline metabolism as the most significant pathway, indicating extensive metabolic disorders during BC progression. Arginine and proline metabolism is a crucial metabolic process responsible for the biosynthesis and conversion of arginine and proline amino acids and their associated intermediates, primarily from glutamate.[39] This metabolic process is essential for cellular nitrogen metabolism and overlaps with other cycles such as the urea and the tricarboxylic acid (TCA) cycles.[39] Recent research emphasizes that the dysregulation of this pathway is a contributory factor in oncogenesis, immune evasion, and reprogramming of metabolism in triple-negative and ILC BC types.[40,41] Consistently, in our study, downregulation of L-arginine, guanidine, *N*-acetylputrescine, urea, and guanidinosuccinic acid was observed in BC patients.

It was previously reported that plasma arginine levels are reduced in early BC, suggesting diminished systemic arginine availability.[42,43] BC cells and tumor-associated immunonuclear cells (e.g., myeloid-derived suppressor cells) were reported to have an increased arginase activity, converting arginine to ornithine and urea. This could result in lowering the systemic arginine concentrations, consistent with decreased plasma L-arginine in cancer patients.[42,43] The depletion of arginine enhances the synthesis of polyamines, which are essential for tumor proliferation.[44] The downregulation of *N*-acetylputrescine, a polyamine catabolite, may also indicate an increased usage of polyamines for proliferation and changed activity of polyamine acetylation and export-related enzymes. The observed decrease in guanidine and guanidinosuccinic acid, both of which are downstream metabolites in the arginine metabolic pathway, further exemplifies this metabolic transition, suggesting that arginine is being preferentially redirected away from its traditional metabolic routes and toward biosynthetic mechanisms that promote tumor advancement. The depletion of arginine not only enhances the synthesis of polyamine, but also inhibits the responses of antitumor T cells, given that T cell proliferation and functionality are significantly dependent on the availability of arginine.[42,43] Arginine was reported to be an epigenetic modulator regulating histone acetylation, resulting in the upregulation of nuclear-encoded oxidative phosphorylation genes.[45]

The noted reduction in urea levels correlates with the process of urea cycle dysregulation in cancer by which nitrogen from catabolic amino acids is diverted away from urea synthesis and directed toward nucleotide and polyamine synthesis.[46] The diversion in this direction sustains the high growth and proliferation needs of cancer cells and leads to decreased circulating levels of urea and its associated metabolites like guanidinosuccinic acid.[46] Overall, these changes highlight a coordinated metabolic adjustment in BC by which cancer

https://doi.org/10.1021/acs.jproteome.5c00669
J. Proteome Res. XXXX, XXX, XXX−XXX

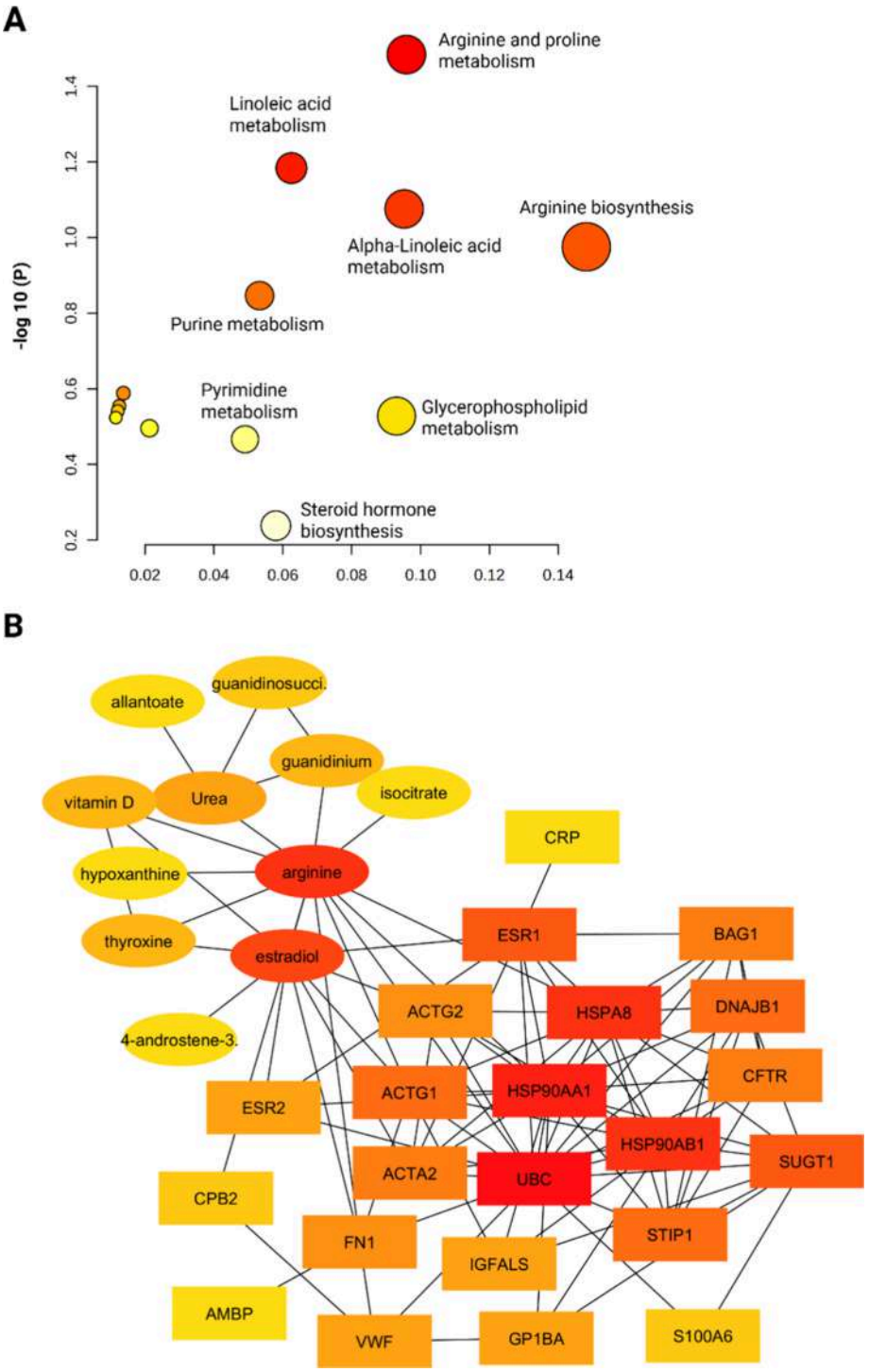

Figure 7. Integrated metabolomics and proteomics analysis. (A) Joint-pathway analysis of the DAMs and DEPs between breast cancer patients and the healthy control. (B) Metabolite−protein interaction network. The diagram illustrates an interaction network connecting metabolites (ellipses) and proteins (rectangles), and nodes are color-coded based on the degree of centrality or importance (from yellow to red).

proliferation as well as immunosuppression in the microenvironment is supported. This provides a rationale by which targeting these pathways (more specifically arginine metabolism) could augment anticancer immunity and provide new therapeutic opportunity.

Lowered plasma arginine and 9-methyluric acid and elevated levels of allantoic acid, hypoxanthine, and uridine in BC patients are consistent with metabolic changes described by the recent multi-omics characterization of endocrine-resistant invasive lobular carcinoma.[40] The study proved that silencing ASS1 induces diminished arginine synthesis and boosts cellular adaptation toward augmented nucleotide metabolism.[40] The upregulation of allantoic acid and hypoxanthine levels in our study probably indicates augmented purine degradation, while increased uridine levels indicate an increase in pyrimidine synthesis. These two processes provide a metabolic support to resistant tumor cells.[40] These findings support the association of arginine starvation and adaptive activation of nucleotide

https://doi.org/10.1021/acs.jproteome.5c00669
J. Proteome Res. XXXX, XXX, XXX−XXX

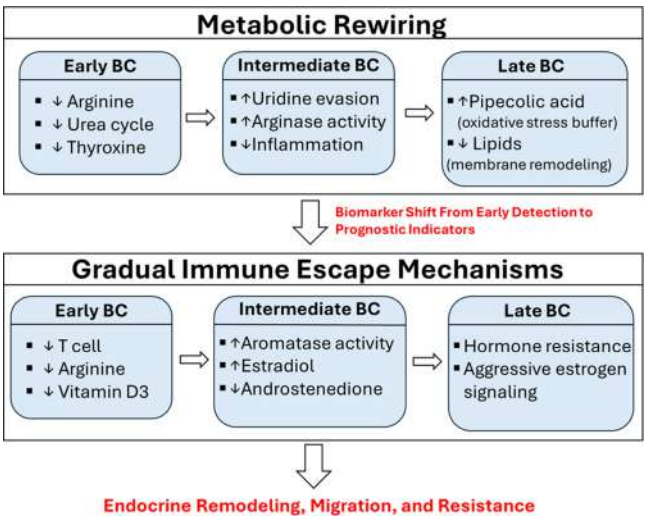

Figure 8. Diagrammatic model illustrating the sequential biological processes occurring during the early stage, the transition phase, and the late stage. This model represents the key metabolic and molecular changes defining each stage, demonstrating the shift from initial pathway activation in the early stage, through intermediate regulatory processes during the transition phase, to the advanced changes characterizing the late-stage progression.

metabolic pathways in endocrine-resistant BC and identify metabolic vulnerabilities that are potentially targetable.[40]

Our results showed a decrease in the levels of vitamin D in BC patients. Various studies demonstrated that vitamin D deficiency is significantly correlated with BC development.[47,48] Vitamin D is reported to enhance the growth of cells and modulate the immune system, and its deficiency has been shown to play a role in tumorigenesis and immune impairment.[49,50] Our results also showed decreased levels of thyroxine (T4), the thyroid gland's primary hormone, which is important to basal metabolic rate control, cell energy production, and cell differentiation.[51] The decreased levels of thyroxine in the plasma of BC patients may indicate its conversion to triiodothyronine (T3). Through its conversion to T3, thyroxine exerts its systemic actions by interacting with nuclear thyroid hormone receptors to modulate target gene transcription.[51] Recent evidence has indicated the role of thyroxine in cancer biology, such as potentially modulating proliferation, angiogenesis, and apoptosis through genomic and nongenomic mechanisms.[51] In BC, thyroxine has been demonstrated to interact with integrin $\alpha v\beta 3$ on the surface of tumor cells driving pro-angiogenesis and cell proliferation.[52] The findings support the need for consideration of thyroid status in BC patients, especially when considering endocrine cross-talk with substances such as vitamin D.

Upregulation of pipecolic acid and estradiol and downregulation of key metabolites such as PC (18:1(9Z)/18:1(9Z)) and androstenedione in the late-stage BC were observed. Increased pipecolic acid levels probably constitute an adaptive mechanism against increased oxidative stress in the tumor microenvironment.[53] The role of pipecolic acid in modulating cellular responses to reactive oxygen species (ROS) and DNA damage has been recently suggested, potentially contributing to cancer cell survival and proliferation under metabolic and genotoxic stress.[53] Increased L-pipecolic acid oxidase (PIPOX) activity, which has been correlated with poor prognosis and metastatic behavior in BC, could further drive this metabolic adaptation.[54] The simultaneous rise in estradiol levels might reflect the multifaceted alteration of estrogen signaling, especially in endocrine-resistant cancers, where estradiol is able to trigger apoptosis or, on the contrary, promote tumor growth through novel routes of ER signaling.[55] Suppressed levels of androstenedione suggest augmented aromatase activity within the tumor microenvironment that enhances the conversion of androstenedione to estradiol.[56] Epigenetic factors were reported to regulate aromatase activity,[57] which was also reported to cross-talk with lipid pathways.[58] Concurrently, downregulation of phosphatidylcholine, PC(18:1(9Z)/18:1-(9Z)), reflects increased membrane biosynthesis and lipid remodeling to support accelerated tumor proliferation.[59]

BC cells exhibit increased biotin demand, which is facilitated by the upregulation of biotin transporters such as the sodium-dependent multivitamin transporter (SMVT; SLC5A6).[60] This enhanced uptake supports rapid tumor proliferation by supplying essential cofactors for carboxylase enzymes involved in key metabolic pathways including fatty acid synthesis and amino acid metabolism.[61] Although tumors consume more biotin, plasma biotin levels may remain stable or even increased due to compensatory mechanisms including hepatic biotin recycling and systemic redistribution.[61] These findings align with metabolomic profiles in BC patients, reflecting a dynamic balance between tumor biotin consumption and overall biotin homeostasis, rather than simple depletion of circulating biotin.[62] This complex regulation underscores the importance of considering whole-body biotin turnover when interpreting plasma biotin concentrations in the context of cancer metabolism and offers insight into the potential therapeutic targeting of biotin transport and metabolism in BC.

The top VIP proteins identified in this study indicate several tumor-associated biological processes relevant to BC progression including coagulation dysregulation, cytoskeletal remodeling, immune modulation, metabolic reprogramming, and growth factor signaling. Alterations in immunoglobulin chains and complement factors reflect immune engagement and localized inflammation.[63,64] Upregulation of the heat shock protein (HSP) and actin was observed in BC patients. HSP and actin regulate the cytoskeletal plasticity required for migration and invasion. HSP90β stabilizes oncogenic kinases and the focal adhesion complex; its pharmacologic inhibition blocks BC metastasis and resensitizes resistant tumors to hormonal therapy.[65,66] In addition, upregulation in protein S100-A6 was observed in our BC patients. S100-A6 was reported to enhance EMT via β-catenin signaling and enhance motility in pancreatic cancer.[67] Angiotensinogen was also upregulated in BC patients compared to in HC individuals. The angiotensinogen/angiotensin II pathway integrates remodeling of the vessels with tumor progression. Angiotensin II through its receptor stimulates proliferation of BC cells, EMT, and angiogenesis,[68,69] while agonistic blockade of the receptors by drugs like losartan has shown antiangiogenic and stromal-normalizing activity in BC models.[70] Apolipoprotein M (component of high-density lipoproteins (HDLs)) was downregulated in BC patients compared to the HC group. Various studies report the downregulation of ApoM in BC tissues, correlating with dysregulated lipid metabolism and aberrant expression of the vitamin D receptor, that can suppress the invasion and progression of tumors.[71]

Together, these alterations reflect a profound reprogramming of amino acid, lipid, and nucleotide metabolism in advanced BC, fueling tumor adaptation and immune evasion yet revealing vulnerabilities that are primed for therapeutic intervention.

https://doi.org/10.1021/acs.jproteome.5c00669
J. Proteome Res. XXXX, XXX, XXX−XXX

4.1. Limitations

Despite the significant results obtained, this study has some limitations including (i) the cohort size (n = 65), which may limit statistical power and generalizability, (ii) the findings are population-specific and may not directly translate to other ethnic or geographic groups, (iii) the observations in this study reflect associations rather than mechanisms, therefore functional validation of identified biomarkers in vitro and in vivo is still required, (iv) the BC cohort may exhibit clinical heterogeneity, including differences in the disease stage and treatment status at the time of sample collection, (v) hormone status and treatment history may have introduced confounding effects, although supplementary analyses indicate that treatment status does not drive the observed molecular patterns, residual confounding cannot be fully excluded, and (vi) diagnostic performance is exploratory since external validation is lacking. Independent validation in external cohorts was not feasible due to the current lack of publicly available BC metabolomic and proteomic data sets from the UAE or comparable regional populations. To mitigate the limitation of the small sample size, stringent quality-control measures and validated statistical approaches were applied. Data reliability was verified through cross-validation and permutation testing to minimize model overfitting. Furthermore, the reproducible trends observed across both univariate and multivariate analyses support the robustness of the findings despite the limited sample size. Future studies should focus on validating these biomarkers in larger, multicenter cohorts, exploring functional roles of key metabolites (e.g., pipecolic acid, estradiol) and proteins in tumor biology, developing noninvasive diagnostic assays based on the identified metabolic signatures, and investigating the therapeutic interventions targeting arginine metabolism, estrogen signaling, and ROS-buffering pathways.

5. CONCLUSIONS

This study provides the first UAE-specific metabolic and proteomic landscape of BC, uncovering a coordinated reprogramming of amino acid, nucleotide, and hormone metabolism across disease stages. The shift from polar to lipophilic metabolites reflects an underlying biological transition tied to tumor proliferation, immune escape, and endocrine resistance. While these findings expand the current understanding of BC biology in an unstudied population, they remain exploratory and correlative. Nevertheless, this work lays the groundwork for precision oncology approaches tailored to the metabolic vulnerabilities of BC in the UAE and potentially other MENA populations.

■ ASSOCIATED CONTENT

Data Availability Statement

The metabolomics data generated in this study is available at the NIH Common Fund's National Metabolomics Data Repository (NMDR) Web site, the Metabolomics Workbench (https://www.metabolomicsworkbench.org) where it has been assigned Study ID ST004098. The data can be accessed directly via its Project DOI: 10.21228/M8XP05.

Supporting Information

The Supporting Information is available free of charge at https://pubs.acs.org/doi/10.1021/acs.jproteome.5c00669.

Metabolic alteration in breast cancer patients compared to control (boxplots showing the relative abundance of significantly different metabolites in early- or late-stage BC compared to HC (FC cutoff 1.5 and q-value <0.05)) (Figure S1); metabolic alteration in breast cancer patients compared to control *continued* (boxplots showing the relative abundance of significantly different metabolites in early- or late-stage BC compared to HC (FC cutoff 1.5 and q-value <0.05)) (Figure S2); the assessment of the effect of treatment using stage-associated biomarkers ((A) the heatmap of selected stage-associated metabolic biomarkers across breast cancer samples; columns represent individual samples and rows represent metabolites identified as stage-associated features; samples are annotated by the treatment category (endocrine-based therapy vs other treatments); (B) the principal component analysis (PCA) score plot based on the same set of stage-associated biomarkers, with samples colored according to the treatment category; PCA demonstrates a substantial overlap between treatment groups, indicating that treatment exposure does not dominate the variance structure of stage-associated metabolic features, and these analyses were performed to evaluate the potential impact of treatment heterogeneity and are interpreted in an exploratory manner) (Figure S3); boxplots of sample intensity distributions following different normalization strategies, including (A) unnormalized $\log_2$-transformed data, (B) global median centering, (C) quantile normalization, (D) Z-score normalization, (E) CV-low subset normalization using empirically invariant features, and (F) housekeeping-based subset normalization using stable plasma proteins and boxplots (Figure S4.); PCA of the data set following different normalization methods, including (A) unnormalized $\log_2$-transformed data, (B) global median centering, (C) quantile normalization, (D) Z-score normalization, (E) subset-focused normalization (PRONE-like approach), and (F) housekeeping-based subset normalization (Figure S5) (PDF)

Accession Codes

The mass spectrometry proteomics data have been deposited to the ProteomeXchange Consortium via the PRIDE (https://www.ebi.ac.uk/pride/) partner repository with the data set identifier PXD067468.

■ AUTHOR INFORMATION

Corresponding Author

Sameh S. M. Soliman − *Research Institute for Medical and Health Sciences and College of Pharmacy, University of Sharjah, Sharjah, United Arab Emirates;* orcid.org/0000-0002-7691-615X; Phone: +971507590985; Email: ssoliman@sharjah.ac.ae

Authors

Sarra B. Shakartalla − *Research Institute for Medical and Health Sciences, University of Sharjah, Sharjah, United Arab Emirates; Faculty of Pharmacy, University of Gezira, Wadmedani, Sudan*

Sara Naif − *Research Institute for Medical and Health Sciences and College of Science, University of Sharjah, Sharjah, United Arab Emirates*

Hamza M. Al-Hroub − *Research Institute for Medical and Health Sciences, University of Sharjah, Sharjah, United Arab Emirates*

https://doi.org/10.1021/acs.jproteome.5c00669
J. Proteome Res. XXXX, XXX, XXX−XXX

Riyad Bendardaf − *College of Medicine, University of Sharjah, Sharjah, United Arab Emirates; Medical Oncology Unit, University Hospital Sharjah, Sharjah, United Arab Emirates*

Complete contact information is available at: https://pubs.acs.org/10.1021/acs.jproteome.5c00669

Funding

This study was funded by the Al Jalila Foundation-Research Grant (Grant No: AJF2023-078) to SSMS.

Notes

The authors declare no competing financial interest.

REFERENCES

(1) WHO *Estimated number of deaths in 2020, world, Females, all ages*; World Health Organization International Agency for Research on Cancer (IARC), 2023. https://gco.iarc.fr/today/online-analysis-pie?v=2020&mode=cancer&mode_population=continents&population=900&populations=900&key=total&sex=2&cancer=39&type=1&statistic=5&prevalence=0&population_group=0&ages_group%5B%5D=0&ages_group%5B%5D=17&nb_items=7&group_cancer=1&include_nmsc=1&include_nmsc_other=1&half_pie=0&donut=0.

(2) Lei, S.; Zheng, R.; Zhang, S.; Wang, S.; Chen, R.; Sun, K.; Zeng, H.; Zhou, J.; Wei, W. Global patterns of breast cancer incidence and mortality: A population-based cancer registry data analysis from 2000 to 2020. *Cancer Communications.* **2021**, *41* (11), 1183.

(3) Soerjomataram, I.; Bray, F. Planning for tomorrow: global cancer incidence and the role of prevention 2020−2070. *Nat. Rev. Clin Oncol.* **2021**, *18* (10), 663.

(4) Radwan, H.; Hasan, H.; Ballout, R. A.; Rizk, R. The epidemiology of cancer in the United Arab Emirates: A systematic review. *Medicine (Baltimore).* **2018**, *97* (50), No. e13618.

(5) Bashir, M. A.; Ali, N. A.; Shaban, S.; Hassouneh, G.; Ashari, M. A.; Jaloudi, M. Young women in the UAE have higher incidence of HER2 positive breast cancer. *Breast J.* **2012**, *18* (6), 637.

(6) Al-Shamsi, H.; Alrawi, S. Breast cancer screening in the United Arab Emirates: is it time to call for a screening at an earlier age. *J. Cancer Prev. Curr. Res.* **2018**, *9* (3), 123.

(7) Al-Shamsi, H. O.; Abdelwahed, N.; Al-Awadhi, A.; Albashir, M.; Abyad, A. M.; Rafii, S.; Afrit, M.; Al Lababidi, B.; Abu-Gheida, I.; Sonawane, Y. P.; Nijhawan, N. A.; Haq, U. U.; Dreier, N.; Joshua, T. L. A.; Iqbal, F.; Yacoub, T.; Nawaz, F. A.; Abdul Jabbar, D.; Tirmazy, S. H.; El-shourbagy, D. M.; Hamza, D.; Omara, M.; Al Madhi, S. A. S.; Ghazal, H.; Darr, H.; Oner, M.; Vlamaki, Z.; El Kinge, A. R.; Ramanathan, D.; Judah, M.; Almahmeed, T.; Ahmad, M.; Jonnada, S. B.; Almansoori, N.; Razek, A. A.; Al-Hamadi, A.; Balalaa, N.; Jamali, F.; Singarachari, R. A.; Labban, A.; Das, K.; Luiten, E. J. T.; Abdelgawad, T.; Al-Khatib, F.; Alrawi, S.; Jaafar, H. Breast Cancer in the United Arab Emirates. *JCO Global Oncol.* **2023**, *9*, No. e2200247.

(8) Najjar, H.; Easson, A. Age at diagnosis of breast cancer in Arab nations. *International Journal of Surgery.* **2010**, *8* (6), 448.

(9) Elobaid, Y.; Aw, T.-C.; Lim, J. N.; Hamid, S.; Grivna, M. Breast cancer presentation delays among Arab and national women in the UAE: a qualitative study. *SSM-population health.* **2016**, *2*, 155.

(10) Alkhatib, M.; Salpini, R.; Carioti, L.; Ambrosio Francesca, A.; D'Anna, S.; Duca, L.; Costa, G.; Bellocchi Maria, C.; Piermatteo, L.; Artese, A.; Santoro Maria, M.; Alcaro, S.; Svicher, V.; Ceccherini-Silberstein, F. Update on SARS-CoV-2 Omicron Variant of Concern and Its Peculiar Mutational Profile. *Microbiol. Spectrum* **2022**, *10* (2), No. e02732-21.

(11) Fiorica, J. V. Breast cancer screening, mammography, and other modalities. *Clinical obstetrics and gynecology.* **2016**, *59* (4), 688.

(12) Bonilla, J. M.; Tabanera, M. T.; Mendoza, L. R. Breast cancer in the 21st century: from early detection to new therapies. *Radiologia* **2017**, *59* (5), 368.

(13) Hanahan, D.; Weinberg, R. A. Hallmarks of cancer: the next generation. *cell.* **2011**, *144* (5), 646.

(14) Kohli, M.; Poulogiannis, G. Harnessing the Power of Metabolomics for Precision Oncology: Current Advances and Future Directions. *Cells.* **2025**, *14* (6), 402.

(15) Wei, Y.; Jasbi, P.; Shi, X.; Turner, C.; Hrovat, J.; Liu, L.; Rabena, Y.; Porter, P.; Gu, H. Early breast cancer detection using untargeted and targeted metabolomics. *Journal of proteome research.* **2021**, *20* (6), 3124.

(16) Xia, J.; Wishart, D. S. Metabolomic data processing, analysis, and interpretation using MetaboAnalyst. *Curr. Protoc. Bioinf.* **2011**, *34* (1), 14.10.1−14.10.48.

(17) Li, L.; Li, R.; Zhou, J.; Zuniga, A.; Stanislaus, A. E.; Wu, Y.; Huan, T.; Zheng, J.; Shi, Y.; Wishart, D. S.; Lin, G. MyCompoundID: Using an Evidence-Based Metabolome Library for Metabolite Identification. *Anal. Chem.* **2013**, *85* (6), 3401.

(18) Cox, J.; Hein, M. Y.; Luber, C. A.; Paron, I.; Nagaraj, N.; Mann, M. Accurate Proteome-wide Label-free Quantification by Delayed Normalization and Maximal Peptide Ratio Extraction, Termed MaxLFQ. *Molecular & Cellular Proteomics.* **2014**, *13* (9), 2513.

(19) Cox, J.; Mann, M. MaxQuant enables high peptide identification rates, individualized p.p.b.-range mass accuracies and proteome-wide protein quantification. *Nat. Biotechnol.* **2008**, *26* (12), 1367.

(20) Tyanova, S.; Temu, T.; Sinitcyn, P.; Carlson, A.; Hein, M. Y.; Geiger, T.; Mann, M.; Cox, J. The Perseus computational platform for comprehensive analysis of (prote)omics data. *Nature Methods.* **2016**, *13* (9), 731.

(21) Dubois, E.; Galindo, A. N.; Dayon, L.; Cominetti, O. Assessing normalization methods in mass spectrometry-based proteome profiling of clinical samples. *Biosystems.* **2022**, *215*−*216*, No. 104661.

(22) Carvalho, L. B.; Teigas-Campos, P. A.; Jorge, S.; Protti, M.; Mercolini, L.; Dhir, R.; Wiśniewski, J. R.; Lodeiro, C.; Santos, H. M.; Capelo, J. L. Normalization methods in mass spectrometry-based analytical proteomics: a case study based on renal cell carcinoma datasets. *Talanta.* **2024**, *266*, No. 124953.

(23) Dressler, F. F.; Brägelmann, J.; Reischl, M.; Perner, S. Normics: Proteomic Normalization by Variance and Data-Inherent Correlation Structure. *Molecular & Cellular Proteomics.* **2022**, *21* (9), No. 100269.

(24) Suo, C.; Salim, A.; Chia, K. S.; Pawitan, Y.; Calza, S. Modified least-variant set normalization for miRNA microarray. *Rna.* **2010**, *16* (12), 2293−303.

(25) Chang, Y.-F. Pipecolic acid pathway: the major lysine metabolic route in the rat brain. *Biochemical and biophysical research communications.* **1976**, *69* (1), 174.

(26) Coradini, D.; Oriana, S. Impact of sex hormones dysregulation and adiposity on the outcome of postmenopausal breast cancer patients. *Clin. Obes.* **2021**, *11* (1), No. e12423.

(27) Chen, C. L.; Hsu, S. C.; Ann, D. K.; Yen, Y.; Kung, H. J. Arginine Signaling and Cancer Metabolism. *Cancers (Basel).* **2021**, *13* (14), 3541.

(28) Yin, J.; Ren, W.; Huang, X.; Deng, J.; Li, T.; Yin, Y. Potential Mechanisms Connecting Purine Metabolism and Cancer Therapy. *Front. Immunol.* **2018**, *9*, 1697.

(29) Wang, W.; Cui, J.; Ma, H.; Lu, W.; Huang, J. Targeting Pyrimidine Metabolism in the Era of Precision Cancer Medicine. *Frontiers in Oncology.* **2021**, *11*, No. 684961.

(30) Juhász, C.; Nahleh, Z.; Zitron, I.; Chugani, D. C.; Janabi, M. Z.; Bandyopadhyay, S.; Ali-Fehmi, R.; Mangner, T. J.; Chakraborty, P. K.; Mittal, S.; Muzik, O. Tryptophan metabolism in breast cancers: molecular imaging and immunohistochemistry studies. *Nuclear Medicine and Biology.* **2012**, *39* (7), 926.

(31) McMahon, A. N.; Reis, I. M.; Takita, C.; Wright, J. L.; Hu, J. J. Metabolomic Profiling of Disease Progression Following Radiotherapy for Breast Cancer. *Cancers (Basel).* **2025**, *17* (5), 891.

(32) Searfoss, R.; Shah, P.; Ofori-Mensa, K.; Bussberg, V.; Tolstikov, V.; Greenwood, B.; Li, H.; Richardson, K.; Miller, G. M.; DeCicco, C.; Granger, E.; Rodrigues, L. O.; Grund, E. M.; Moser, A. J.; Sarangarajan, R.; Narain, N. R.; Kiebish, M. A. Impact of hemolysis on multi-OMIC pancreatic biomarker discovery to derisk biomarker development in precision medicine studies. *Sci. Rep.* **2022**, *12* (1), 1186.

(33) Lang, B. J.; Guerrero, M. E.; Prince, T. L.; Okusha, Y.; Bonorino, C.; Calderwood, S. K. The functions and regulation of heat shock

proteins; key orchestrators of proteostasis and the heat shock response. *Archives of toxicology.* **2021**, *95* (6), 1943.
(34) Ganguly, S.; Naik, D.; Muskara, A.; Mian, O. Y. The Nexus of Endocrine Signaling and Cancer: How Steroid Hormones Influence Genomic Stability. *Endocrinology* **2021**, *162* (1), No. bqaa177.
(35) Giretti, M. S.; Simoncini, T. Rapid regulatory actions of sex steroids on cell movement through the actin cytoskeleton. *Steroids.* **2008**, *73* (9−10), 895−900.
(36) Stournaras, C.; Gravanis, A.; Margioris, A. N.; Lang, F. The actin cytoskeleton in rapid steroid hormone actions. *Cytoskeleton.* **2014**, *71* (5), 285.
(37) Donnelly, T. T.; Hwang, J. Breast cancer screening interventions for Arabic women: a literature review. *Journal of Immigrant and Minority Health.* **2015**, *17* (3), 925.
(38) Han, J.; Li, Q.; Chen, Y.; Yang, Y. Recent Metabolomics Analysis in Tumor Metabolism Reprogramming. *Frontiers in Molecular Biosciences.* **2021**, *8*, No. 763902.
(39) Wang, D.; Duan, J. J.; Guo, Y. F.; Chen, J. J.; Chen, T. Q.; Wang, J.; Yu, S. C. Targeting the glutamine-arginine-proline metabolism axis in cancer. *J. Enzyme Inhib. Med. Chem.* **2024**, *39* (1), No. 2367129.
(40) Gupta, A.; Choueiry, F.; Reardon, J.; Pramod, N.; Kulkarni, A.; Shankar, E.; Sizemore, S. T.; Stover, D. G.; Zhu, J.; Ramaswamy, B.; Majumder, S. Invasive lobular carcinoma: integrated multi-omics analysis reveals silencing of Argininosuccinate synthase and upregulation of nucleotide biosynthesis in tamoxifen resistance. *Cell Death Dis.* **2025**, *16* (1), 514.
(41) García, L. S.; Quintas, G.; Hernández, M. P.; Martínez, D. C.; Torregosa, M. D.; Marín, S.; Mancino, M.; O'Connor Blasco, J. E.; Llombart-Cussac, A.; Fernández-Murga, M. L. The immune and metabolic profile in the response to neoadjuvant treatment with immune checkpoint inhibitors in triple-negative breast cancer patients. *Cancer Res.* **2025**, *85* (8_Supplement_1), 5799.
(42) Vissers, Y. L.; Dejong, C. H.; Luiking, Y. C.; Fearon, K. C.; von Meyenfeldt, M. F.; Deutz, N. E. Plasma arginine concentrations are reduced in cancer patients: evidence for arginine deficiency? *American journal of clinical nutrition.* **2005**, *81* (5), 1142.
(43) Engelen, M.; Klimberg, V. S.; Allasia, A.; Deutz, N. E. P. Major surgery diminishes systemic arginine availability and suppresses nitric oxide response to feeding in patients with early stage breast cancer. *Clinical Nutrition.* **2018**, *37* (5), 1645.
(44) Liu, R.; Li, P.; Bi, C. W.; Ma, R.; Yin, Y.; Bi, K.; Li, Q. Plasma N-acetylputrescine, cadaverine and 1,3-diaminopropane: potential biomarkers of lung cancer used to evaluate the efficacy of anticancer drugs. *Oncotarget.* **2017**, *8* (51), 88575.
(45) Chen, C.-L.; Hsu, S.-C.; Chung, T.-Y.; Chu, C.-Y.; Wang, H.-J.; Hsiao, P.-W.; Yeh, S.-D.; Ann, D. K.; Yen, Y.; Kung, H.-J. Arginine is an epigenetic regulator targeting TEAD4 to modulate OXPHOS in prostate cancer cells. *Nat. Commun.* **2021**, *12* (1), 2398.
(46) Lee, J. S.; Adler, L.; Karathia, H.; Carmel, N.; Rabinovich, S.; Auslander, N.; Keshet, R.; Stettner, N.; Silberman, A.; Agemy, L.; Helbling, D.; Eilam, R.; Sun, Q.; Brandis, A.; Malitsky, S.; Itkin, M.; Weiss, H.; Pinto, S.; Kalaora, S.; Levy, R.; Barnea, E.; Admon, A.; Dimmock, D.; Stern-Ginossar, N.; Scherz, A.; Nagamani, S. C. S.; Unda, M.; Wilson, D. M., 3rd; Elhasid, R.; Carracedo, A.; Samuels, Y.; Hannenhalli, S.; Ruppin, E.; Erez, A. Urea Cycle Dysregulation Generates Clinically Relevant Genomic and Biochemical Signatures. *Cell* **2018**, *174* (6), 1559.
(47) Eliassen, A. H.; Warner, E. T.; Rosner, B.; Collins, L. C.; Beck, A. H.; Quintana, L. M.; Tamimi, R. M.; Hankinson, S. E. Plasma 25-hydroxyvitamin D and risk of breast cancer in women followed over 20 years. *Cancer research.* **2016**, *76* (18), 5423.
(48) Mackey, J. D.; Young, P.; Zimmerer, R.; Miles, B. Vitamin D deficiency as a risk factor for breast cancer development. *Journal of Clinical Oncology.* **2023**, *41*, 10559.
(49) Daryabor, G.; Gholijani, N.; Kahmini, F. R. A review of the critical role of vitamin D axis on the immune system. *Experimental and Molecular Pathology.* **2023**, *132*, No. 104866.
(50) Samuel, S.; Sitrin, M. D. Vitamin D's role in cell proliferation and differentiation. *Nutr. Rev.* **2008**, *66* (suppl_2), S116.
(51) Krashin, E.; Piekiełko-Witkowska, A.; Ellis, M.; Ashur-Fabian, O. Thyroid hormones and cancer: a comprehensive review of preclinical and clinical studies. *Front. Endocrinol.* **2019**, *10*, 59.
(52) Davis, P. J.; Glinsky, G. V.; Lin, H.-Y.; Leith, J. T.; Hercbergs, A.; Tang, H.-Y.; Ashur-Fabian, O.; Incerpi, S.; Mousa, S. A. Cancer cell gene expression modulated from plasma membrane integrin $\alpha v\beta 3$ by thyroid hormone and nanoparticulate tetrac. *Front. Endocrinol.* **2015**, *5*, 240.
(53) Liu, L.; Wu, J.; Shi, M.; Wang, F.; Lu, H.; Liu, J.; Chen, W.; Yu, G.; Liu, D.; Yang, J.; Luo, Q.; Ni, Y.; Jin, X.; Jin, X.; Chen, W. L. New Metabolic Alterations and A Predictive Marker Pipecolic Acid in Sera for Esophageal Squamous Cell Carcinoma. *Genomics Proteomics Bioinformatics.* **2022**, *20* (4), 670.
(54) Cha, Y. J.; Kim, D. H.; Jung, W. H.; Koo, J. S. Expression of sarcosine metabolism-related proteins according to metastatic site in breast cancer. *Int. J. Clin. Exp. Pathol.* **2014**, *7* (11), 7824.
(55) Kota, K.; Brufsky, A.; Oesterreich, S.; Lee, A. Estradiol as a Targeted, Late-Line Therapy in Metastatic Breast Cancer with Estrogen Receptor Amplification. *Cureus* **2017**, *9* (7), No. e1434.
(56) Chatterton, R. T. Functions of dehydroepiandrosterone in relation to breast cancer. *Steroids.* **2022**, *179*, No. 108970.
(57) Izawa, M.; Harada, T.; Taniguchi, F.; Ohama, Y.; Takenaka, Y.; Terakawa, N. An epigenetic disorder may cause aberrant expression of aromatase gene in endometriotic stromal cells. *Fertility and sterility.* **2008**, *89* (5), 1390.
(58) Subbaramaiah, K.; Howe, L. R.; Bhardwaj, P.; Du, B.; Gravaghi, C.; Yantiss, R. K.; Zhou, X. K.; Blaho, V. A.; Hla, T.; Yang, P.; et al. Obesity is associated with inflammation and elevated aromatase expression in the mouse mammary gland. *Cancer Prev. Res.* **2011**, *4* (3), 329.
(59) Saito, R. F.; Andrade, L. N. S.; Bustos, S. O.; Chammas, R. Phosphatidylcholine-Derived Lipid Mediators: The Crosstalk Between Cancer Cells and Immune Cells. *Frontiers in Immunology.* **2022**, *13*, No. 768606.
(60) Vadlapudi, A. D.; Vadlapatla, R. K.; Pal, D.; Mitra, A. K. Biotin uptake by T47D breast cancer cells: functional and molecular evidence of sodium-dependent multivitamin transporter (SMVT). *International journal of pharmaceutics.* **2013**, *441* (1−2), 535.
(61) Wang, C.; Xiu, Y.; Zhang, Y.; Wang, Y.; Xu, J.; Yu, W.; Xing, D. Recent advances in biotin-based therapeutic agents for cancer therapy. *Nanoscale.* **2025**, *17* (4), 1812.
(62) Perry, C. A.; Butterick, T. A. *Biotin. Advances in Nutrition.* **2024**, *15* (7), No. 100251.
(63) Cui, M.; Huang, J.; Zhang, S.; Liu, Q.; Liao, Q.; Qiu, X. Immunoglobulin Expression in Cancer Cells and Its Critical Roles in Tumorigenesis. *Frontiers in Immunology.* **2021**, *12*, No. 613530.
(64) Markiewski, M. M.; Lambris, J. D. The role of complement in inflammatory diseases from behind the scenes into the spotlight. *American Journal of Pathology.* **2007**, *171* (3), 715−27.
(65) Li, Z. N.; Luo, Y. HSP90 inhibitors and cancer: Prospects for use in targeted therapies (Review). *Oncol. Rep.* **2023**, *49* (1), 6.
(66) Whitesell, L.; Santagata, S.; Mendillo, M. L.; Lin, N. U.; Proia, D. A.; Lindquist, S. HSP90 empowers evolution of resistance to hormonal therapy in human breast cancer models. *Proceedings of the National Academy of Sciences.* **2014**, *111* (51), 18297.
(67) Chen, X.; Liu, X.; Lang, H.; Zhang, S.; Luo, Y.; Zhang, J. S100 calcium-binding protein A6 promotes epithelial-mesenchymal transition through β-catenin in pancreatic cancer cell line. *PLoS One.* **2015**, *10* (3), No. e0121319.
(68) Oh, E.; Kim, J. Y.; Cho, Y.; An, H.; Lee, N.; Jo, H.; Ban, C.; Seo, J. H. Overexpression of angiotensin II type 1 receptor in breast cancer cells induces epithelial-mesenchymal transition and promotes tumor growth and angiogenesis. *Biochim. Biophys. Acta* **2016**, *1863* (6 Pt A), 1071−1081.
(69) Alamro, A. A.; Almutlaq, M. A.; Alghamdi, A. A.; Alshammari, A. H.; Alshehri, E.; Abdi, S. Role of Renin-Angiotensin System and Macrophages in Breast Cancer Microenvironment. *Diseases* **2025**, *13* (7), 216.

https://doi.org/10.1021/acs.jproteome.5c00669
J. Proteome Res. XXXX, XXX, XXX−XXX

(70) Coulson, R.; Liew, S. H.; Connelly, A. A.; Yee, N. S.; Deb, S.; Kumar, B.; Vargas, A. C.; O'Toole, S. A.; Parslow, A. C.; Poh, A.; Putoczki, T.; Morrow, R. J.; Alorro, M.; Lazarus, K. A.; Yeap, E. F. W.; Walton, K. L.; Harrison, C. A.; Hannan, N. J.; George, A. J.; Clyne, C. D.; Ernst, M.; Allen, A. M.; Chand, A. L. The angiotensin receptor blocker, Losartan, inhibits mammary tumor development and progression to invasive carcinoma. *Oncotarget.* **2017**, *8* (12), 18640−56.

(71) Zhou, Y.; Luo, G. Apolipoproteins, as the carrier proteins for lipids, are involved in the development of breast cancer. *Clinical & Translational Oncology.* **2020**, *22* (11), 1952.

https://doi.org/10.1021/acs.jproteome.5c00669
J. Proteome Res. XXXX, XXX, XXX−XXX